ADVANCED SCIENCE Open Access
www.advancedscience.com

Discovery of a Small Molecule Activator of Slack (Kcnt1) Potassium Channels That Significantly Reduces Scratching in Mouse Models of Histamine-Independent and Chronic Itch

Annika Balzulat, W. Felix Zhu, Cathrin Flauaus, Victor Hernandez-Olmos, Jan Heering, Sunesh Sethumadhavan, Mariam Dubiel, Annika Frank, Amelie Menge, Maureen Hebchen, Katharina Metzner, Ruirui Lu, Robert Lukowski, Peter Ruth, Stefan Knapp, Susanne Müller, Dieter Steinhilber, Inga Hänelt, Holger Stark, Ewgenij Proschak, and Achim Schmidtko**

Various disorders are accompanied by histamine-independent itching, which is often resistant to the currently available therapies. Here, it is reported that the pharmacological activation of Slack (Kcnt1, $K_{Na}1.1$), a potassium channel highly expressed in itch-sensitive sensory neurons, has therapeutic potential for the treatment of itching. Based on the Slack-activating antipsychotic drug, loxapine, a series of new derivatives with improved pharmacodynamic and pharmacokinetic profiles is designed that enables to validate Slack as a pharmacological target in vivo. One of these new Slack activators, compound 6, exhibits negligible dopamine D_2 and D_3 receptor binding, unlike loxapine. Notably, compound 6 displays potent on-target antipruritic activity in multiple mouse models of acute histamine-independent and chronic itch without motor side effects. These properties make compound 6 a lead molecule for the development of new antipruritic therapies targeting Slack.

1. Introduction

Itching (also known as pruritus) is defined as an unpleasant sensation that evokes a desire to scratch. Depending on whether histamine release is involved, itching can be broadly divided into histamine-dependent (histaminergic) and histamine-independent (non-histaminergic) itching.[1–3] Like pain, acute itching serves as an important protective mechanism for detecting potentially harmful stimuli. However, chronic itch (i.e., persisting for more than 6 weeks in humans) no longer serves a useful function but instead imposes suffering and may compromise the quality of life to a degree often comparable to that seen in chronic pain.[4] Chronic itch is a debilitating symptom that accompanies various

A. Balzulat, C. Flauaus, M. Hebchen, K. Metzner, R. Lu, A. Schmidtko
Institute of Pharmacology and Clinical Pharmacy
Goethe University Frankfurt
Max-von-Laue-Str. 9, 60438 Frankfurt am Main, Germany
E-mail: schmidtko@em.uni-frankfurt.de

W. F. Zhu, A. Menge, S. Knapp, S. Müller, D. Steinhilber, E. Proschak
Institute of Pharmaceutical Chemistry
Goethe University Frankfurt
Max-von-Laue-Str. 9, 60438 Frankfurt am Main, Germany
E-mail: proschak@pharmchem.uni-frankfurt.de

V. Hernandez-Olmos, J. Heering, D. Steinhilber, E. Proschak
Fraunhofer Institute for Translational Medicine and Pharmacology ITMP
Theodor-Stern-Kai 7, 60596 Frankfurt am Main, Germany

S. Sethumadhavan, I. Hänelt
Institute of Biochemistry
Goethe University Frankfurt
Max-von-Laue-Str. 9, 60438 Frankfurt am Main, Germany

M. Dubiel, A. Frank, H. Stark
Institute of Pharmaceutical and Medicinal Chemistry
Heinrich Heine University Düsseldorf
Universitätsstr. 1, 40225 Düsseldorf, Germany

A. Menge, S. Knapp, S. Müller
Structural Genomics Consortium (SGC)
Buchmann Institute for Molecular Life Sciences
Goethe University Frankfurt
Max-von-Laue-Str. 15, 60438 Frankfurt am Main, Germany

R. Lukowski, P. Ruth
Department of Pharmacology
Toxicology and Clinical Pharmacy
Institute of Pharmacy University of Tübingen
Auf der Morgenstelle 8, 72076 Tübingen, Germany

The ORCID identification number(s) for the author(s) of this article can be found under https://doi.org/10.1002/advs.202307237

DOI: 10.1002/advs.202307237

skin disorders, systemic diseases, such as chronic kidney or cholestatic liver disease, psychiatric diseases, and neuropathies, or is idiopathic. An estimated one third of dermatology patients and nearly 15% of the general population experience chronic itching.[5–7] As most types of chronic itch are histamine-independent and, therefore, resistant to antihistamines, there is an urgent need to develop novel treatment strategies.[8]

Most known mechanisms of pruriception (itching sensation) begin with the activation of itch-sensitive sensory neurons. Several key receptors, including members of the Mas-related G-protein-coupled receptor (Mrgpr) families, are important for detecting non-histaminergic chemical itch signals.[2,9] Recent single-cell RNA-sequencing (scRNA-seq) studies have revealed that itch-related genes are highly expressed in distinct subpopulations of sensory neurons. For example, in a pioneering scRNA-seq study by Usoskin et al.,[10] 11 principal types of sensory neurons were identified, of which three non-peptidergic populations (NP1, NP2, and NP3) were proposed to be itch-sensitive. After activation, these sensory neurons signal to the dorsal horn of the spinal cord, where ongoing information is further processed and transmitted to itch-signaling pathways ascending to the brain.[11]

The excitability of sensory neurons is driven by various types of ion channels, among which K^+ channels are the most diverse class governed by more than 75 genes in humans. Owing to their diversity and tissue-dependent expression patterns, they are increasingly recognized as potential drug targets.[12,13] Notably, the K^+ channel Slack (also known as $K_{Na}1.1$ or Slo2.2; gene *Kcnt1*), which is activated by intracellular Na^+ and inhibited by bivalent cations,[14–16] is highly enriched in the itch-sensitive NP1, NP2, and NP3 subsets of sensory neurons of the peripheral nervous system in mice[10,17] (Figure S1A,B, Supporting Information), suggesting that Slack has a role in itch. In fact, a remarkable functional role of Slack in pruriception is reflected by the increased scratching behavior of Slack knockout mice after exposure to pruritogens such as chloroquine.[18] These findings in combination with the observation that Slack expression in non-human primate sensory neurons (Figure S1C, Supporting Information) and human sensory neurons (Figure S1D, Supporting Information) is enriched in itch-associated cell populations[19,20] support the hypothesis that pharmacological activators of Slack hold therapeutic potential for the treatment of itch.

A previous study with a library screen of pharmacologically active compounds reported that the first-generation antipsychotic drug loxapine activates Slack.[21] Interestingly, in preliminary experiments, we observed that systemic administration of a low dose of loxapine considerably alleviated chloroquine-induced scratching behavior in wildtype mice but did not affect scratching behavior in Slack knockout mice, indicating that the loxapine-induced antipruritic effect depends on Slack activation. However, the clinical use of loxapine is limited by the typical adverse events associated with first-generation antipsychotic drugs, which are mainly caused by the blocking of dopamine receptors and other neurotransmitter receptors.[22,23] Hence, in this study, we aimed to develop novel Slack-activating compounds with an improved pharmacological profile as compared to that of loxapine, in particular by reducing off-target activity toward dopamine receptors. We hypothesized that these aims could be achieved by introducing modifications to the loxapine scaffold. Using these new compounds, we aimed to validate Slack as a novel target for itch treatment.

2. Results

2.1. Development of Slack-Activating Compounds

We developed a series of 114 new derivatives of loxapine. The new compounds were synthesized using linear synthesis routes (Figure S2, Supporting Information). Their structural features are listed in **Table 1**. The loxapine scaffold contains a tricyclic core and a piperazine ring substituted with an alkyl residue. Starting from methyl esters of salicylic acid and 2-fluoronitrobenzene derivatives, diarylethers were obtained via nucleophilic aromatic substitution. Subsequent reduction of the nitro group by tin(II)chloride enabled intramolecular amide bond formation. Alternatively, an amide bond was first formed between 2-fluorobenzoic acids and 2-aminophenol derivatives, followed by intramolecular nucleophilic aromatic substitution to afford the same lactam core. The lactam was then converted to the imidoyl chloride using $POCl_3$. In the final step, the substituted piperazines displaced the chloride to afford the desired loxapine derivatives.

The functional activity of this series of compounds against human Slack was determined using a cell-based FluxOR potassium ion channel assay in cultured HEK293 cells stably expressing human Slack (herein referred to as HEK-Slack cells) and a Na^+-free assay buffer to prevent compound-independent Slack activation by monovalent cations.[14,24] Having established that the FluxOR assay is capable to detect Slack activation by loxapine (Figure S3, Supporting Information), we conducted concentration-response experiments to determine the EC_{50} and E_{MAX} values. Of the 114 newly synthesized compounds, 31 acted as Slack activators to varying extents. Accordingly, we deemed eight of these as the most interesting candidates. Their Slack-activating properties are listed in Table 1. Potency (EC_{50}) values ranged between 3.2 and 62.5 μM, whereas loxapine activated Slack with a potency of 20.7 μM (Table 1 and **Figure 1A**). Efficacy (E_{MAX}) values ranged from 63.1% to 222.8% normalized to Slack activation by loxapine (Table 1 and Figure 1A). Considering that low doses of loxapine exerted Slack-dependent effects in mice,[24] we concluded that the potency of these eight new compounds may be sufficient to activate Slack at standard doses in vivo.

The evaluation of analogs in our series of Slack activators in the FluxOR assay suggested that the replacement of the chloro substituent at R^1 by a trifluoromethyl group improved activity (compound 1). The additional introduction of a fluoro substituent at the other aryl ring (R^2) increased efficacy but reduced potency (compound 3). In some cases, the sulfur analogs showed comparable activity (compound 5). Replacement of piperazine with homopiperazine improved the EC_{50} value but decreased the E_{MAX} value (compound 2). Modification of the alkyl residue at R^3 was generally better tolerated and had the potential to tune the Slack activity and pharmacological properties. Derivatives with aliphatic hydroxy groups exhibited good efficacy, with acceptable EC_{50} values (compound 4). Finally, an ionizable carboxyl group could be incorporated only at a specific linker length (compound 6), because both the addition and removal of another ethoxy unit resulted in a complete loss of activity. The combination of

Table 1. Structural features of the most promising new compounds and their Slack-activating properties. The chemical synthesis scheme of the new compounds is depicted in Figure S2 (Supporting Information). Potency (EC_{50}) and efficacy (E_{MAX}; % relative to loxapine) values are from a FluxOR assay in HEK-Slack cells, shown in Figure 1A. New compounds were measured in triplicate. EC_{50} and E_{MAX} values are presented as mean with a 95% confidence interval.

	Substituents	R^1	R^2	R^3	X	n	FluxOR assay	
	Activator						EC_{50} [μM]	E_{MAX} [%]
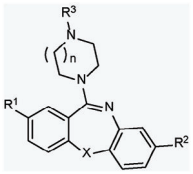	Loxapine	Cl	H		O	1	20.7 (16.3–26.4)	100
	1	CF_3	H		O	1	6.3 (5.3–7.4)	114.3 (101.0–127.6)
	2	CF_3	H		O	2	3.2 (2.3–4.5)	63.1 (55.0–71.3)
	3	CF_3	F		O	1	41.5 (36.2–47.6)	199.1 (174.8–223.4)
	4	Cl	H		O	1	26.0 (21.7–31.1)	222.8 (193.6–252.0)
	5	Cl	H	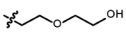	S	1	30.0 (23.9–37.7)	87.4 (73.9–101.0)
	6	Cl	H	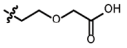	O	1	30.3 (20.8–44.1)	96.2 (72.4–120.0)
	7	CF_3	H	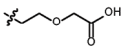	O	1	62.5 (49.3–79.2)	177.0 (138.7–215.3)
	8	CF_3	H	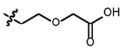	O	2	50.9 (46.0–56.3)	186.4 (169.7–203.2)

advantageous structural motifs did not result in a cumulative gain of activity, as compounds 7 and 8 showed improved efficacy but worse potency.

Next, we verified Slack activation by the new compounds using whole-cell patch-clamp recordings in HEK-Slack cells. Experiments were performed with a Na^+-free pipette solution. In each series of experiments, compounds were added to the external solution at a concentration of 50 μM, and loxapine at a concentration of 50 μM was used as a positive control whereas vehicle (0.03% DMSO) served as a solvent control. At a holding potential of −70 mV, a series of 500 ms-long test pulses ranging from −120 to +120 mV in intervals of 20 mV were applied.[16] Our patch-clamp recordings revealed that the developed Slack activators (except compound 2) significantly increased the I_K amplitude compared to the vehicle (Figure 1B; Figure S4, Supporting Information). At a voltage of +80 mV, the current densities of the compounds increased with a range between 2.0- and 14.8-fold compared to the baseline (Figure 1B). Notably, the efficacy of our compounds in patch-clamp recordings (i.e., the fold increase in current density) markedly correlated with their efficacy in the FluxOR assay (Figure 1C). Together, our FluxOR assay and patch-clamp analyses in HEK-Slack cells indicated that these new compounds activate Slack in vitro.

2.2. In Vitro Characterization of New Slack Activators

To explore whether the compounds affected general cell functions, we performed a live-cell high-content assay that allowed for the simultaneous investigation of cellular viability, compound precipitation, and maintenance of membrane integrity and mitochondrial mass.[25] HEK293 cells were stained with multiple dyes and incubated with the new compounds or loxapine at different concentrations (0.1–100 μM), and the fluorescence and cellular shape were analyzed after 6 h. We found that none of the compounds induced a relevant cytotoxic effect or affected membrane integrity, and compound precipitation was only detected for compound 1 at 100 μM whereas an increase in mitochondrial mass by more than 50% was detected only for compound 8 at 100 μM (Figure S5A–D, Supporting Information). Similarly, low cytotoxicity was observed in HEK-Slack cells, which were incubated with the compounds and analyzed by brightfield microscopy after 24 h (Figure S5E, Supporting Information). Together, these data suggest that general cell functions are not affected by any of our new compounds at concentrations up to 50 μM.

We next assessed the metabolic stability of these compounds (10 μM) in rat liver microsomes (**Figure 2A**). In this assay, loxapine was metabolized rapidly, with only 6% of the drug remaining unmodified after 15 min. The known metabolites of loxapine include amoxapine, 7-OH-loxapine, 8-OH-loxapine, and loxapine N-oxide.[26] Therefore, we assumed that the occupation of metabolically labile sites at the aromatic core and the reduction in electron density at the oxidizable nitrogen atom of the piperazine ring might increase metabolic stability. Indeed, both the introduction of fluorine at R^2 and the introduction of an electron-withdrawing carboxylic acid linker at R^3 improved metabolic stability. The substitution of chlorine with a trifluoromethyl group at R^1 was also beneficial. In contrast, homopiperazine and hydroxy linkers were metabolically labile. Compounds 6 and 7 exhibited the highest metabolic stabilities in vitro.

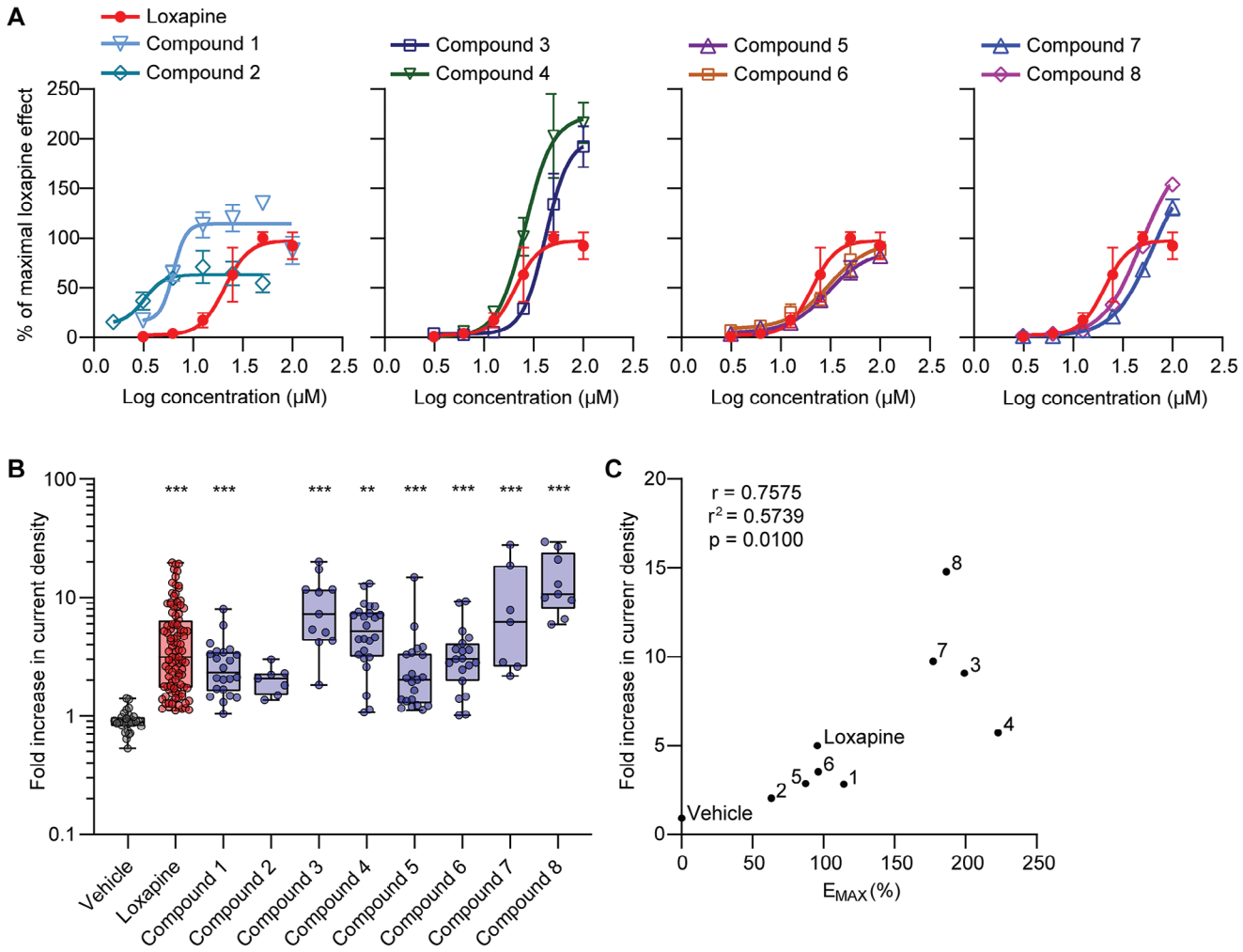

Figure 1. Compounds serving as activators of Slack channels. A) Concentration-response experiments with our new compounds in the FluxOR potassium ion channel assay. HEK293 cells stably expressing human Slack (HEK-Slack cells) were assayed for a potassium channel-mediated thallium response using FluxOR. Each compound was incubated at six concentrations in a Na^+-free assay buffer to prevent compound-independent Slack activation by monovalent cations.[14,24] For each sample, the fluorescence value was calculated and then normalized to the maximum fluorescence value of loxapine. For better comparability, data from the loxapine measurements are presented in all four graphs. Each data point is the average of three replicates. Data represent the mean ± SD. The resulting EC_{50} and E_{MAX} values from these measurements are shown in Table 1. Representative traces from FluxOR experiments are presented in Figure S3H,I (Supporting Information). B) Patch-clamp recordings confirm that new compounds evoke Slack-mediated potassium currents. Whole-cell voltage recordings on HEK-Slack cells were performed using a Na^+-free pipette solution at baseline and after incubation with a new compound (50 μM), loxapine (50 μM), or vehicle (external solution containing 0.03% DMSO). Loxapine was incubated in each series of experiments as a positive control. Shown is the fold increase in current densities (pA/pF) elicited by new compounds, loxapine, and vehicle relative to baseline at a voltage of +80 mV (vehicle, $n = 28$ cells; loxapine, $n = 104$; compound 1, $n = 22$; compound 2, $n = 7$; compound 3, $n = 10$; compound 4, $n = 24$; compound 5, $n = 21$; compound 6, $n = 19$; compound 7, $n = 7$; compound 8, $n = 9$; $^{**}p < 0.01$, $^{***}p < 0.001$ versus vehicle; Kruskal–Wallis test with Dunn's correction. Box-and-whisker plots represent maximum and minimum values, and the box shows the first, second (median), and third quartile values. Current-voltage curves from these recordings are presented in Figure S4 (Supporting Information). C) Correlation of relative E_{MAX} values of new compounds obtained in the FluxOR assay (presented in A and Table 1) with relative current densities obtained in the patch-clamp experiments (presented in B). Statistical significance was assessed by a Pearson correlation.

Because some of the most limiting adverse effects of loxapine are mediated by the antagonism of dopamine receptors, we aimed to develop derivatives with decreased dopamine receptor affinity. Therefore, we determined the binding affinities of our compounds to D_2 and D_3 dopamine receptors using a [^{3}H]-spiperone displacement assay (Figure 2B; Table S1, Supporting Information). As expected, loxapine displayed pronounced binding to the D_2 and D_3 receptors, with K_i values of 32 and 112 nM, respectively. Generally, the affinity was further promoted by the trifluoromethyl group at R^1. Derivatives with a homopiperazine ring or hydroxy linker had a slightly lower affinity. Importantly, compound 6 exhibited a ≈40-fold lower affinity against D_2 and a ≈31-fold lower affinity against D_3 as compared to loxapine. These findings prompted us to focus on compound 6 for the remainder of this study.

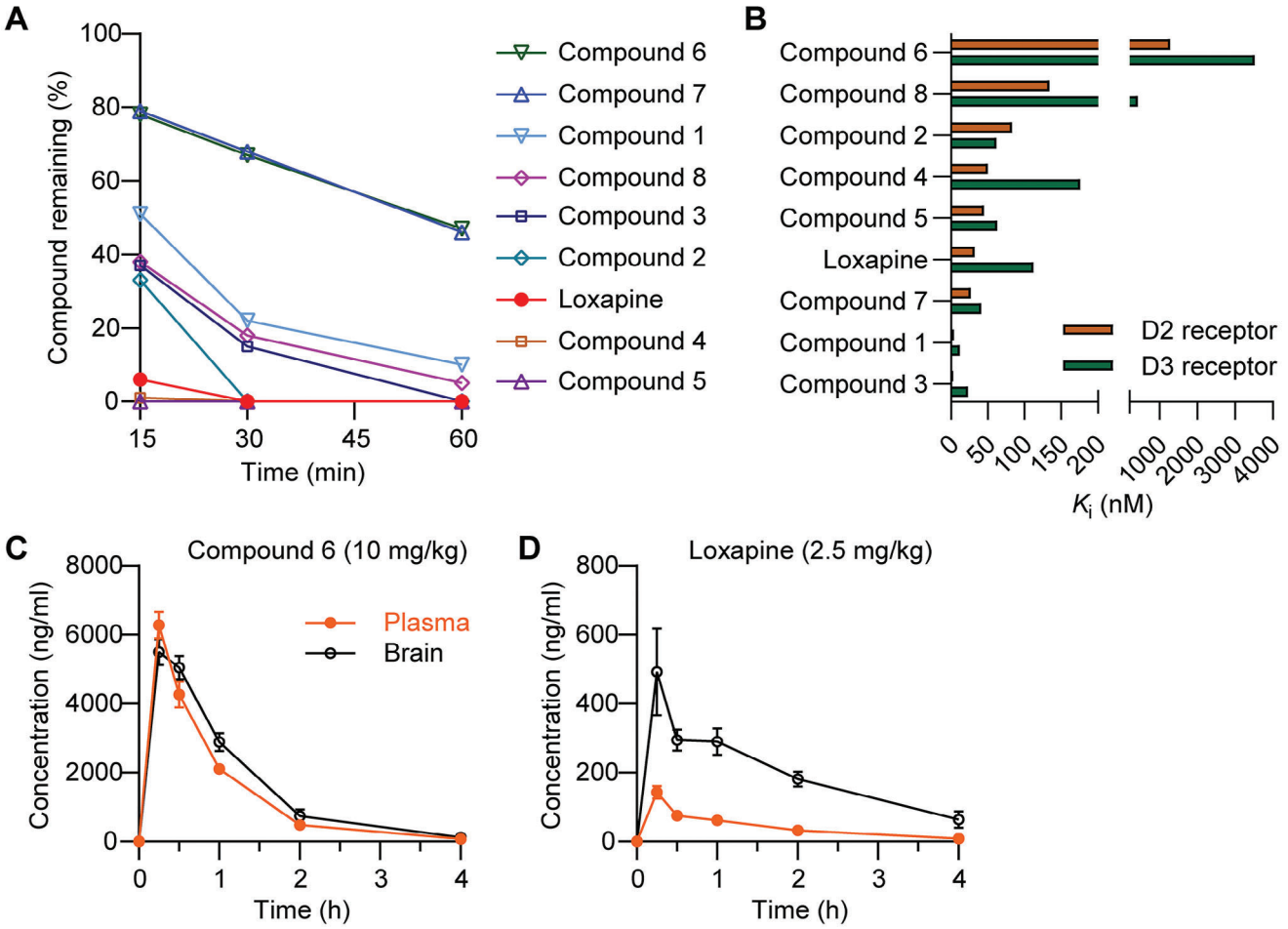

Figure 2. In vitro characterization of the new compounds and pharmacokinetics of compound 6. A) Phase I metabolism of our new compounds was assessed using a microsomal stability assay in rat liver microsomes. The percentage of compound remaining was measured 15, 30, and 60 min after compound exposure (10 μM). Data are expressed as the mean ± SEM of the remaining compound from three independent experiments. B) Affinity at D_2 and D_3 receptors of our new compounds was determined in a [^{3}H]-Spiperone competition binding assay using a cell membrane preparation of CHO cells stably expressing the human D_{2S} and D_3 receptor. Data represent the mean; the 95% confidence interval and *n* number are presented in Table S1 (Supporting Information). Data in (A) and (B) show that compound 6 has a high microsomal stability and a low affinity to D_2 and D_3 receptors. C,D) Pharmacokinetic properties of compound 6 in comparison to loxapine. Animals were i.p. injected with 10 mg kg^{-1} compound 6 (C) or 2.5 mg kg^{-1} loxapine (D) and plasma and brain levels were measured at the indicated time points by LC-MS analysis. Data are presented as mean ± SEM of three mice per group. Additional pharmacokinetic parameters are presented in Table S2 (Supporting Information).

2.3. Target Binding and Off-Target Profile of Compound 6

To confirm that the cellular effect of compound 6 was mediated by its direct interaction with Slack, ligand binding on purified human Slack (Figure S6A, Supporting Information) was assessed by differential scanning fluorimetry (DSF), thereby evaluating a ligand-dependent shift of the protein melting temperature (T_m). The cysteine-reacting dye 7-diethylamino-3-(4-maleimidophenyl)−4-methylcoumarin (CPM), which binds to cysteine residues that are accessible during protein unfolding, was used as an indicator for protein unfolding. In the absence of ligand, Slack had a T_m of 30 °C. In the presence of a Slack inhibitor (compound 31 from ref. [27]), known to directly interact with the protein and therefore used as a positive control, T_m saturated at 45.7 ± 3.2 °C at a ligand concentration of 100 μM (Figure S6B, Supporting Information), indicating a notable stabilization of Slack. Similarly, protein unfolding with compound 6 and loxapine reached its maximum at 100 μM ligand concentration with T_ms of 39.3 ± 0.9 and 37.8 ± 1.3 °C, respectively, reflecting an increase in T_m of 9.3 and 7.8 °C, respectively. These results confirmed that compound 6 and loxapine acted as direct ligands on Slack (Figure S6B, Supporting Information).

To estimate whether compound 6 is an opener and/or a gating modulator of Slack, we analyzed how intracellular Na^+ affects its potency. Whole-cell patch-clamp recordings in HEK-Slack cells were performed using pipette solutions with either 0 or 10 mM Na^+.[18] In a Na^+-free pipette solution, incubation with compound 6 at a concentration of 25 μM increased the current densities compared to baseline. Interestingly, with a 10 mM pipette Na^+, the increase in current densities evoked by compound 6 was more pronounced compared to the vehicle (Figure S7, Supporting Information). These data in combination with the

electrophysiology experiments in Figure 1B suggest that compound 6 acts as a true opener (that works in the absence of Na^+) and a gating modulator (that is more potent in the presence of intracellular Na^+) of Slack.

As loxapine is a first-generation antipsychotic with a substantial binding affinity for many receptors,[26] we next explored the pharmacological profile of compound 6 and loxapine in vitro using a SafetyScreen44 panel (Eurofins), which measures the interaction of compounds with 44 targets. In this panel, loxapine (10 μM) showed substantial binding inhibition (higher than 50%) for 17 out of 44 targets including adrenergic (α_{1A} and α_{2A}), dopamine (D_1 and D_{2S}), histamine (H_1 and H_2), muscarinic (M_1, M_2, and M_3), and serotonin (5-HT_{1A}, 5-HT_{1B}, 5-HT_{2A}, 5-HT_{2B}, and 5-HT_3) receptors; Na^+ channel; norepinephrine transporter (NET); and serotonin transporter (SET) (Figure S8, Supporting Information), thereby confirming the "dirty" nature of first-generation antipsychotics. Of note, considerably less off-target activities were observed for compound 6 (10 μM), which exhibited substantial binding to 8 targets (α_{1A}, D_1, D_{2S}, H_1, 5-HT_{2A}, 5-HT_{2B}, NET, and SET). These data suggested an improved pharmacological profile of compound 6 compared to that of loxapine. Furthermore, compound 6 (like loxapine) did not measurably bind to human ether-à-go-go (hERG) or voltage-gated (K_V) potassium channels in the off-target screen (Figure S8, Supporting Information), suggesting that this compound does not act as an unspecific modulator of potassium channels.

2.4. Compound 6 Profoundly Inhibits Itch-Related Behavior in Mice

To prepare for in vivo studies, we investigated the pharmacokinetic properties of compound 6. Following intraperitoneal (i.p.) administration of compound 6 (10 mg kg^{-1}) in mice, plasma and brain levels were determined over 4 h using LC-MS. We found that compound 6 concentrations decayed with first-order kinetics in the plasma and brain, with a half-life of ≈35 min, and readily crossed the blood–brain barrier (Figure 2C; Table S2, Supporting Information). No obvious impairment of mouse behavior was observed after the administration of compound 6 at this dose. For comparison, we determined the plasma and brain loxapine levels. As i.p. administration of 10 or 5 mg kg^{-1} loxapine caused obvious signs of toxicity (i.e., considerably reduced activity), loxapine was administered at a dose of 2.5 mg kg^{-1}. Relatively low concentrations of loxapine were detected in the plasma (Figure 2D; Table S2, Supporting Information), which was consistent with its rapid metabolism (Figure 2A).[28] Moreover, loxapine had an especially high brain exposure ($ratio_{brain/plasma}$ = 5.12) which is in accordance with its activity on dopamine receptors in the central nervous system (CNS), unlike compound 6 (Figure 2B). Collectively, the pharmacological and pharmacokinetic profiles of compound 6 make it an excellent molecule for in vivo pharmacodynamic studies.

The in vivo efficacy of compound 6 was analyzed in mice of both sexes, and no significant sex-related differences were observed in the behavioral experiments (Figures S9 and S10, Supporting Information). As a prerequisite for interpreting itch behavior experiments, we first tested motor function after systemic dosing. Treatment with compound 6 (3–30 mg i.p.) did not impair motor function in the accelerating rotarod test, a standard model of motor performance (**Figure 3A**), or in the vertical pole test, which assesses basal ganglia-related movement disorders (Figure 3B). By contrast, loxapine at a dose of ≥ 0.39 mg kg^{-1} markedly reduced the ability of the mice to perform in both models (Figure 3A,B), which is in line with its high CNS penetration and dopamine receptor affinity, thereby confirming earlier reports.[24]

We then assessed the antipruritic efficacy of compound 6 in a model of histamine-independent itching induced by the antimalarial drug chloroquine. Importantly, we found that systemic treatment of mice with compound 6 (3, 10, or 30 mg kg^{-1} i.p.) 15 min prior to subcutaneous (s.c.) injection of chloroquine into the nape of the neck ameliorated scratching behavior in a dose-dependent manner (Figure 3C). Further experiments supported the conclusion that the antipruritic effects were mediated by Slack activation because compound 6 did not significantly alter chloroquine-induced scratching in animals with a genetic deletion of Slack ($Slack^{-/-}$ mice; Figure 3D). Taken together, these data suggest that treatment with compound 6 ameliorates chloroquine-induced itching by activating Slack.

Chloroquine-induced scratching in mice is driven by MrgprA3 activation in the NP2 population of sensory neurons.[10,29] To further explore the antipruritic efficacy of compound 6 in histamine-independent itch, we assessed the behavioral response after s.c. injection of the peptide Ser-Leu-Ile-Gly-Arg-Leu (SLIGRL) that evokes scratching by activation of MrgprC11,[30] which is expressed in the NP2 and NP3 population.[10] Similar to the chloroquine model, compound 6 (10 mg kg^{-1} i.p.) significantly inhibited SLIGRL-induced scratching behavior (Figure 3E). Moreover, compound 6 ameliorated histamine-independent itch evoked by s.c. injection of β-alanine that activates MrgprD[31] in the NP1 population of sensory neurons[10] (Figure 3F). In contrast, scratching induced by subcutaneous histamine was not affected by compound 6 (Figure 3G). The lack of an effect on histamine-evoked scratching was supported by the low affinity of compound 6 for histamine H_1 receptors, which was determined using a [^{3}H]-pyrilamine competition binding assay in vitro (Table S3, Supporting Information). In addition, the unaltered scratching behavior in the histamine model provided further evidence that the effects of compound 6 observed in the histamine-independent models did not result from impaired motor function. We also investigated the efficacy of compound 6 after peroral (p.o.) delivery. Consistent with the relatively high exposure after oral dosing (Table S2, Supporting Information), this molecule also conferred a profound antipruritic effect when delivered at a dose of 15 mg kg^{-1} p.o. in the chloroquine itch model (Figure 3H).

We next assessed the efficacy of compound 6 in the treatment of chronic itching. In a model of allergic contact dermatitis,[32] applying the hapten 2,4-dinitrofluorobenzene (DNFB) to the nape of the neck twice two weeks apart (**Figure 4A**) resulted in persistent itching behavior reflected by scratching the painted area and head-shaking, which was significantly correlated with scratching (Figure S10E–G, Supporting Information). Interestingly, compound 6 administered i.p. after the second DNFB exposure significantly reduced the number of scratching bouts and head shakes

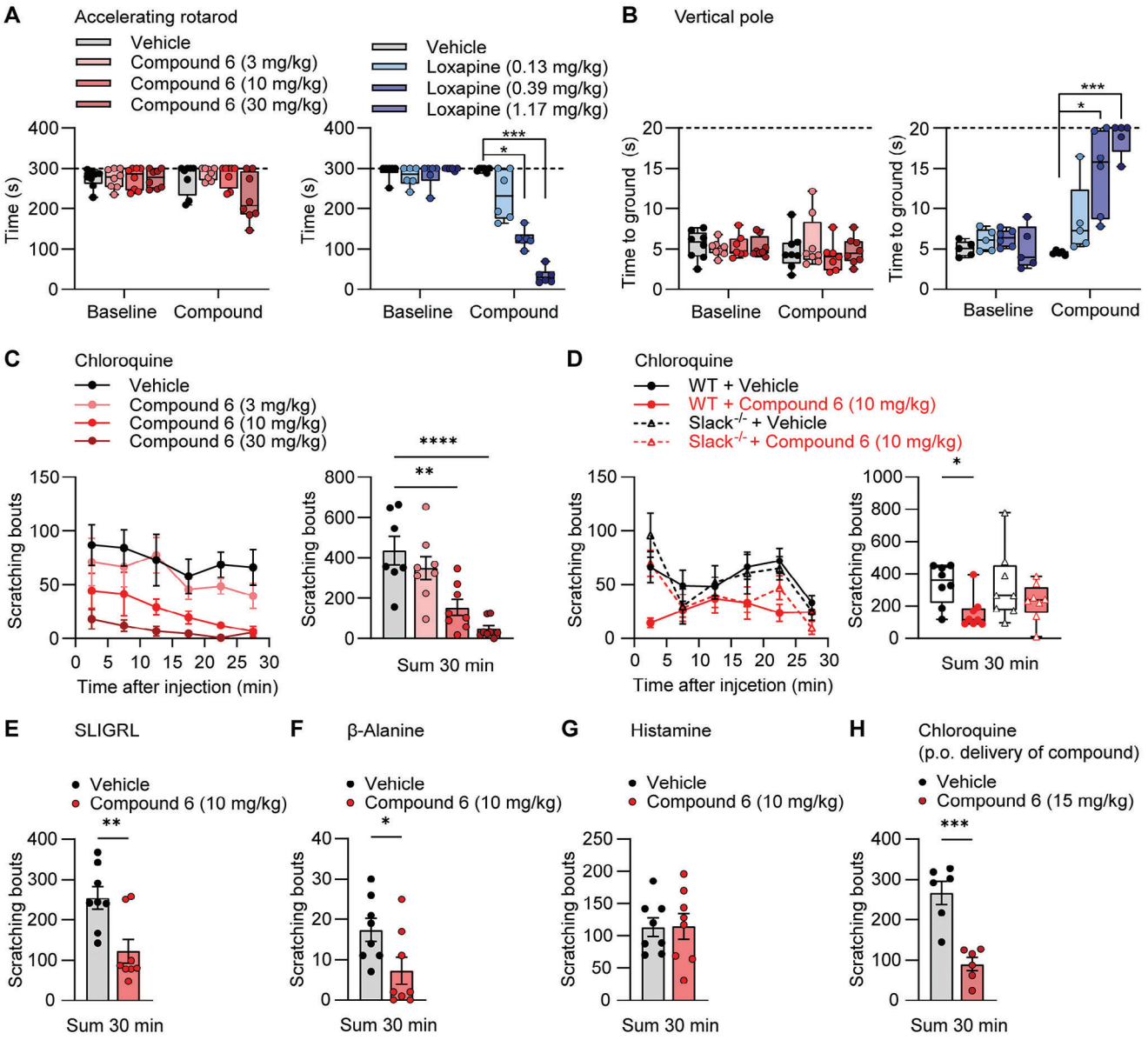

Figure 3. Compound 6 inhibits histamine-independent acute itch behavior. A,B) Motor function. Compound 6, loxapine or vehicle (0.9% NaCl with 10% 2-hydroxypropyl-β-cyclodextrine) were i.p. administered, and an accelerating rotarod test (A) followed by a vertical pole test (B) was performed 15 min thereafter. Data show that compound 6 did not affect the time spent on the rotarod or the vertical pole, whereas loxapine dose-dependently inhibited motor coordination in both models. Box-and-whisker plots represent maximum and minimum values, and the box shows the first, second (median), and third quartile values. Dotted lines indicate cutoff times ($n = 6$–8). $^{*}p < 0.05$, $^{***}p < 0.001$, Kruskal–Wallis test. C,D) Chloroquine-induced itch behavior. Compound 6 or vehicle were i.p. administered. After 15 min, chloroquine was s.c. administered into the nape of the neck and the number of scratching bouts was counted over 30 min. In each panel, the time course of scratching behavior is shown on the left and the sum of scratching bouts in 30 min is presented on the right. Note that compound 6 inhibited the scratching behavior induced by chloroquine in a dose-dependent manner (C) and that compound 6 significantly inhibited the chloroquine-induced scratching behavior in WT mice but not in Slack$^{-/-}$ littermates (D). In C, data represent the mean ± SEM (n = 7–8). Vehicle (veh) versus 3 mg kg^{-1}, $p = 0.4713$; veh versus 10 mg kg^{-1}, $p = 0.0013$; veh versus 30 mg kg^{-1}, $p = < 0.0001$; one-way-ANOVA with Dunnett's correction. In D, data in the time course diagram represent the mean ± SEM; data in the sum diagram are presented as box-and-whisker plots with maximum and minimum values, in which the box shows the first, second (median), and third quartile values ($n = 8$). WT (veh vs compound 6), $p = 0.0242$; Slack$^{-/-}$ (veh vs compound 6), $p > 0.9999$; Kruskal–Wallis test with Dunn's correction. E–G) Itch behavior induced by SLIGRL, β-alanine or histamine. Compound 6 significantly ameliorated the scratching behavior induced by SLIGRL (E) or β-alanine (F), but not by histamine (G). Data represent the mean ± SEM ($n = 8$). $p = 0.0053$ (E), $p = 0.0365$ (F), $p = 0.9563$ (G); unpaired Student's t-test. H) Acute itch behavior in the chloroquine model was also inhibited after p.o. administration of compound 6 under similar experimental settings as in C but with p.o. delivery of compound 6 or vehicle. Data represent the mean ± SEM ($n = 6$). $p = 0.0004$; unpaired Student's t-test. $^{*}p < 0.05$, $^{**}p < 0.01$, $^{***}p < 0.001$, $^{****}p < 0.0001$.

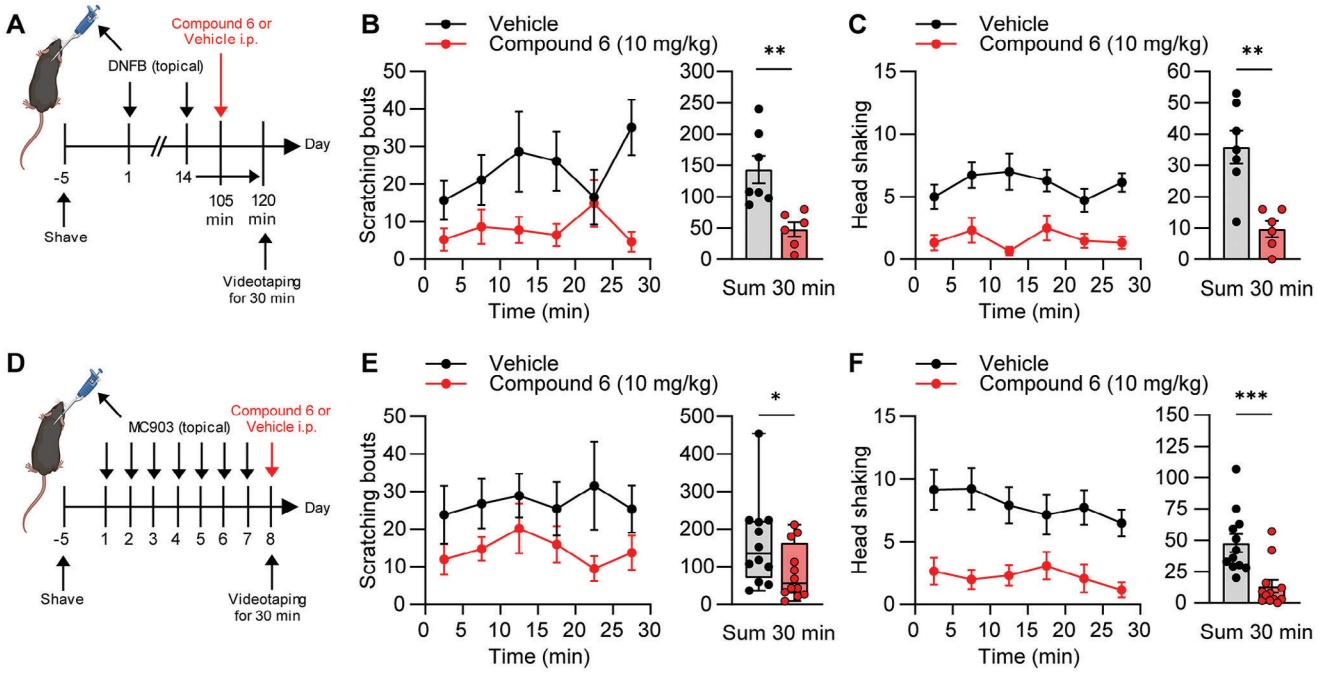

Figure 4. Compound 6 inhibits persistent itch behavior. A–C) Efficacy of compound 6 in the DNFB model of persistent itch. A) Experimental diagram showing the induction of spontaneous itch behavior by topical application of 2,4-dinitrofluorobenzene (DNFB) to the nape of the neck (twice 14 days apart), i.p. drug delivery 105 min after the second DNFB application, and videotaping 15 min thereafter. Compound 6 significantly reduced the number of scratching bouts (B) and the number of head shakes (C) as compared to vehicle. Data are presented as mean ± SEM ($n = 6$–7). $p = 0.004$, unpaired Student's *t*-test (B); $p = 0.0014$, unpaired Student's *t*-test (C). D–F) Efficacy of compound 6 in the MC903 model of persistent itch. D) Experimental diagram showing the induction of spontaneous scratching by topical application of MC903 to the nape of the neck (once daily over 7 days), i.p. drug delivery at day 8, and videotaping 15 min thereafter. In comparison to the vehicle, compound 6 significantly reduced the number of scratching bouts (E) and the number of head shakes (F). In E, box-and-whisker plots represent maximum and minimum values, and the box shows the first, second (median), and third quartile values. All other data are presented as mean ± SEM ($n = 12$). $p = 0.0319$, Mann–Whitney test (E); $p = 0.0008$, unpaired Student's *t*-test (F);. $^{*}p < 0.05$, $^{**}p < 0.01$, $^{***}p < 0.001$. Schemes in A and D were created with BioRender.com.

compared to vehicle-treated animals (Figure 4B,C). Similarly, in the MC903 model of skin inflammation (Figure 4D), which has some characteristics of allergic contact dermatitis and atopic dermatitis,[33,34] compound 6 significantly ameliorated scratching and head shaking (Figure 4E,F). These findings are important because they indicate that Slack activators can reduce existing itching.

Finally, compound 6 was screened for potential side effects in vivo. In pulse oximetry measurements of conscious, freely moving mice, i.p. administration of compound 6 (10 mg kg^{-1}) did not affect the heart rate (Figure S11A, Supporting Information) or breath rate (Figure S11B, Supporting Information) during an observation period of 30 min. In contrast, both parameters were reduced after i.p. administration of morphine (10 mg kg^{-1}), which was used as a positive control in this experiment. Because Slack-positive sensory neurons are polymodal and involved in the sensation of mechanical and heat stimuli,[35] we also tested the response to mechanical (von Frey filament test) and thermal (Hargreaves test) stimulation of the hindpaws after i.p. administration of compound 6 (10 mg kg^{-1}). Neither mechanical nor thermal sensitivity was altered by compound 6 compared to the vehicle control (Figure S11C,D, Supporting Information). Taken together, these results highlight that compound 6 effectively inhibited the itch behavior of mice in multiple models at a well-tolerated dose.

2.5. Compound 6 Inhibits Itch-Sensitive Sensory Neurons

To determine whether the antipruritic effect of compound 6 occurs directly at the neuronal level, we used whole-cell patch-clamp electrophysiology to measure the excitability of sensory neurons. In order to simulate a pathological state, we incubated dorsal root ganglia (DRG) neuronal cultures with an "inflammatory soup" (histamine: 10 µM, PGE_2: 10 µM, serotonin: 10 µM, bradykinin: 10 µM)[36] overnight and performed recordings on cells that bind isolectin B4 (IB4), a marker of non-peptidergic C-fiber neurons including the itch-sensitive neuronal populations (NP1–NP3)[10] in mice. Neurons from these cultures displayed pronounced hyperexcitability, as indicated by action potential (AP) firing after the current injection (200–950 pA; **Figure 5A**). Notably, the application of compound 6 (50 µM), but not of vehicle, caused a profound decrease in the number of AP fired (Figure 5A,B). Neither compound 6 nor the vehicle significantly affected the resting membrane potential (RMP; Figure 5B). Next, we examined APs evoked by injection of small currents (0–220 pA) in the sensitized (i.e., after incubation with "inflammatory soup") IB4-binding neurons (Figure 5C). In these recordings, some cells elicited APs with 0 pA current injection, whereas in other cells APs were evoked after current injections above 0 pA. Of note, in the presence of compound 6, only 7 of 13 cells elicited APs, whereas in the presence of vehicle, all (11 of 11) cells

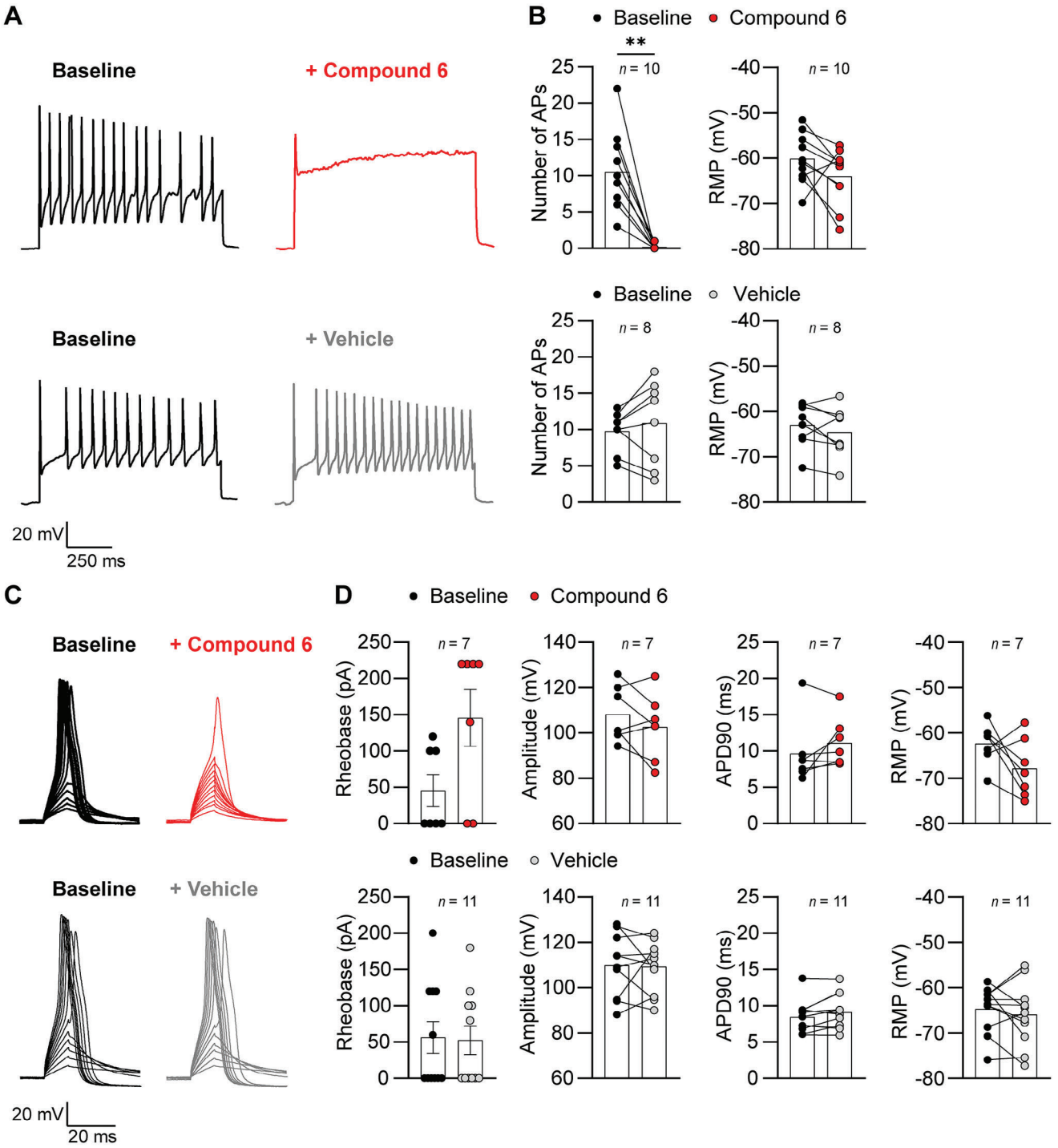

Figure 5. Compound 6 reduces the neuronal excitability of itch-sensitive sensory neurons. DRG neurons were incubated overnight with an "inflammatory soup" followed by whole-cell current-clamp recordings on IB4-binding neurons. A) Representative recording from a neuron showing action potential (AP) firing in response to current injections (200–950 pA at 150 pA intervals, 1000-ms duration) at baseline and in the presence of compound 6 (50 μM) or vehicle. Shown are representative traces at a current injection of 350 pA (compound 6) and 650 pA (vehicle). B) Group data show that compound 6 significantly inhibited the number of APs compared to baseline but did not significantly affect the resting membrane potential (RMP). Baseline versus compound 6: number of APs, $p = 0.0020$, Wilcoxon test ($n = 10$); RMP, $p = 0.1061$, paired Student's t-test ($n = 10$). Baseline versus vehicle: number of APs, $p = 0.3912$, paired Student's t-test ($n = 8$); RMP, $p = 0.2391$, paired Student's t-test ($n = 8$). C) Representative recordings from neurons after injections of small currents (0–220 pA at 20 pA intervals, 10-ms duration) at baseline and in the presence of compound 6 (50 μM) or vehicle. The representative traces show that in the presence of compound 6 the AP initiations failed with lower current injections and only 1 AP was evoked with the highest current injection, whereas in the presence of the vehicle, APs were evoked already at lower current injections. D) Group data from the experiment

elicited APs. This observation further supports the finding that compound 6 reduces the excitability of sensory neurons. Moreover, in the 7 cells in which APs were recorded in the presence of compound 6, the rheobase (i.e., the current required to generate an AP) was visibly, but not significantly, increased compared to baseline (Figure 5D). In contrast, the rheobase remained unchanged after the application of the vehicle (Figure 5D). Neither compound 6 nor the vehicle had a significant effect on AP amplitude, AP duration at 90% repolarization (APD90), or RMP in the cells with recorded APs (Figure 5D). As compound 6 inhibited the formation of APs in the latter experiments, we explored whether this effect might be related to an off-target binding to voltage-dependent Na^+ channels. However, compound 6 (50 μM) did not affect tetrodotoxin-resistant Na^+ currents in IB4-binding sensory neurons (Figure S12, Supporting Information). Together, these findings confirmed that the Slack-activating compound 6 inhibited itch-sensitive sensory neurons in mice.

3. Discussion

The research presented here identifies several new compounds that can activate Slack channels. Our finding that the lead molecule, compound 6, effectively inhibited scratching elicited by multiple histamine-independent pruritogens in mice established Slack activation as a novel pharmacological strategy for the treatment of antihistamine-resistant itch.

Our aim to develop Slack-activating compounds for the treatment of itch was based on the finding that Slack expression is enriched in all subtypes of itch-sensing sensory neurons (Figure S1, Supporting Information) and that Slack controls the bursting and adaptation of action potential firing rates, thereby reducing the neuronal activity of sensory neurons.[24,37–39] We started compound optimization from an approved drug, which is considered to be a highly favorable approach known as selective optimization of side activities (SOSA).[40,41] Loxapine has been previously discovered as a Slack activator,[21] however the pharmacodynamic properties of loxapine clearly limit its applicability in patients.[23] Moreover, the lack of selectivity toward key aminergic receptors prevents the applicability of loxapine as a reliable pharmacological tool to validate Slack as a therapeutic target. In the case of the loxapine-derivative compound 6, the replacement of the methyl residue by the negatively charged ethoxyacetic acid moiety led to a substantial reduction in off-target interactions, while the efficacy and potency of Slack activation were similar to those of loxapine. Overall, these properties qualify compound 6 as a valuable pharmacological tool for investigating the effects of Slack activation in vivo. Indeed, the profound inhibition of scratching behavior in mice after administration of compound 6 (10–30 mg kg^{-1}) suggests that this compound sufficiently activates Slack in vivo, although its FluxOR EC_{50} value (30 μM) is relatively high. When interpreting the FluxOR EC_{50} values, it should be considered that the assay buffer in our FluxOR measurements was Na^+-free, which might cause a lower potency of compound 6 in these in vitro experiments compared to the in vivo studies. This assumption is supported by our patch-clamp recordings in HEK-Slack cells that revealed a higher increase in current density in the presence of 10 mM intracellular Na^+. Moreover, the FluxOR experiments were performed using an assay buffer containing 2 mM Ca^{2+}. A previous study revealed that Ca^{2+} inhibits Slack activity with an IC_{50} of 0.26 mM when applied to the intracellular side of the membrane in inside-out patches.[15] Although highly speculative, the EC_{50} values measured in our FluxOR assay may have been affected by Ca^{2+}-mediated Slack inhibition, which might be more pronounced in the Na^+-free assay buffer of this in vitro approach. It should be also noted that the FluxOR assay is a Tl^+-based surrogate ion assay. It is well established that the surrogate ions have different permeabilities compared to physiologic ions, which may cause a right shift of potency values.[42] Furthermore, the plasma protein binding and tissue binding of compound 6 in vivo needs to be considered when comparing the in vitro EC_{50} values and the in vivo efficacy, because according to the free drug hypothesis, it is the free drug that distributes into the extravascular space and is responsible for both efficacy and toxicity. Nevertheless, the assumption that Slack is the primary target mediating antipruritic activity in vivo is supported by the observation that the action of compound 6 was largely abolished in $Slack^{-/-}$ mice. Based on the hits in the off-target screen, it might be possible that the binding of compound 6 to $5HT_{2A}$ receptors also affects its antipruritic efficacy because serotonin causes itching via the activation of several 5-HT receptors, most commonly $5\text{-}HT_2$ (ref. [43]). $5\text{-}HT_{2A}$ (but not $5\text{-}HT_{2B}$) is expressed in sensory neurons.[44] It must be taken into account, however, that in our off-target screen, the compounds were incubated at only one concentration (10 μM). Determination of receptor affinities will be important in future studies to further explore the extent of off-target interactions.

We found that compound 6 inhibited the scratching behavior of mice in the chloroquine, SLIGRL, and β-alanine model of acute non-histaminergic itch and in the DNFB and MC903 model of chronic itch. Furthermore, compound 6 profoundly inhibited the excitability of IB4-binding sensory neurons in mice. The strong efficacy of compound 6 in mice, together with the prominent expression of Slack in pruritogen receptor-enriched sensory neurons in humans (Figure S1D, Supporting Information), suggests that Slack activators may also be effective for the treatment of itch in humans. However, it should be considered that the mechanisms underlying itch sensation and processing in humans are poorly understood. Moreover, there are substantial

with small current injections. In these recordings, some cells elicited APs with 0 pA injection, whereas other cells elicited APs after a current injection above 0 pA. In the presence of compound 6, APs were recorded in only 7 of 13 cells, whereas in the presence of a vehicle, APs were recorded in 11 of 11 cells. In the cells with evoked APs, the rheobase was visibly, but not significantly, increased in the presence of compound 6 ($p = 0.0625$, Wilcoxon test, $n = 7$) and was unchanged in the presence of vehicle ($p = 0.6250$, Wilcoxon test, $n = 11$). The AP amplitude, the AP duration at 90% repolarization (APD90), and the RMP were not significantly altered in the presence of compound 6 or vehicle (baseline versus compound 6: amplitude, $p = 0.1946$, paired Student's t-test ($n = 7$); APD90, $p = 0.2117$, paired Student's t-test ($n = 7$); RMP, $p = 0.1175$, paired Student's t-test ($n = 7$). Baseline versus vehicle: amplitude, $p = 0.8838$, paired Student's t-test ($n = 11$); APD90, $p = 0.0649$, paired Student's t-test ($n = 11$); RMP, $p = 0.4446$, paired Student's t-test ($n = 11$). The single point data in B and D represent the individual responses to compound 6 or vehicle compared to the baseline in each cell, the bars indicate the mean (mean ± SEM for rheobase). $^{**}p < 0.01$.

differences in the expression of itch-relevant genes between species. For example, mice express 27 Mrgprs, whereas humans express eight Mrgprs (MRGPRX1–X4 and MRGPRD–G). MRGPRX1, -X4, and -D are expressed in the human DRG and trigeminal ganglia and have been implicated in non-histaminergic itch as receptors for pruritic compounds.[45] Further studies are needed to elucidate the functional role of Slack in the human itch sensation.

Although we did not extensively evaluate the side effects, we found that motor coordination (Figure 3A,B), heart rate or breathing rate (Figure S11A,B, Supporting Information), and the sensing of mechanical or thermal stimuli (Figure S11C,D, Supporting Information) were not affected by the administration of compound 6 at an effective antipruritic dose. With regard to the safety profile, it should be considered that Slack is expressed in various neuronal populations in the CNS, and gain-of-function mutations of *KCNT1* have been associated with epileptic encephalopathies in humans.[46] Limited information exists concerning the incidence of seizures during loxapine treatment. The overall risk for loxapine-induced seizures seems to be low at therapeutic doses,[22,26] but it should be used with caution in patients with a history of convulsive disorders. In our behavioral studies in mice, we did not observe any overt signs of seizures after the systemic administration of compound 6 at doses up to 30 mg kg^{-1}. However, the epileptogenic potential of brain-penetrant Slack activators such as compound 6 should be carefully assessed in the future.

In summary, compound 6 represents a new family of Slack activators. Its profound efficacy in various itch models illustrates its potential as an antipruritic drug for the treatment of histamine-independent and chronic itch.

4. Experimental Section

Chemicals/Drugs: Loxapine, pregabalin, chloroquine, SLIGRL-NH_2, β-alanine, histamine, PGE_2, serotonin, and bradykinin were purchased from Sigma–Aldrich (Munich, Germany). All indicated concentrations refer to those of pure substances. Reagents and solvents for the synthesis of loxapine derivatives were obtained from Acros Organics (Gel, Belgium), Alfa Aesar GmbH & Co KG (Karlsruhe, Germany), BLDPharm Inc. (NuiNan, China), Fluorochem Ltd. (Hadfield, UK), Sigma–Aldrich, and TCI Europe N.V. (Zwijndrecht, Belgium).

Design, Preparation, and Analytical Characterization of Loxapine Derivatives: Reactions were carried out in an argon atmosphere. NMR spectra were recorded on Bruker DPX250, Bruker Avance 300, Bruker Avance 400, or Bruker Avance 500 (Bruker, Karlsruhe, Germany) operating at ambient temperature. Proton spectra were recorded in $CDCl_3$ or DMSO-d_6, and ^1H NMR chemical shifts were referenced to the residual signals of $CHCl_3$ (at $\delta = 7.26$ ppm) and DMSO-d_5 (at $\delta = 2.50$ ppm). ^{13}C NMR chemical shifts were referenced against the central line of the solvent signal (for $CHCl_3$ at $\delta = 77.16$ ppm and for DMSO-d_6 at $\delta = 39.52$ ppm). Chemical shifts are given on δ scale (ppm). The coupling constants (J) are given in hertz (Hz). The multiplicities are as follows: s (singlet), d (doublet), t (triplet), q (quartet), quint or m (multiplet). ESI-MS was performed with an LCMS-2020 from Shimadzu and HRMS with a MALDI Orbitrap XL (Thermo Scientific). TLC was carried out on silica gel plates from Marcherey-Nagel (ALUGRAM) and visualized with a UV lamp (254 nm and/or 366 nm). Purification of products was performed by flash chromatography using puriFlash XS420 and Silica HP 30 µm columns as stationary phase (Interchim, Montluçon, France). Analytical and semi-preparative HPLC was conducted using Shimadzu Prominence with an SPD20A UV/Vis detector (Shimadzu, Duisburg, Germany). Stationary phases were Luna 10 µm 100 Å, C18(2) (250×4.6 mm), and Luna 10 µm 100 Å, C18(2) (250×21.20 mm), from Phenomenex (Aschaffenburg, Germany), and the eluent was a mixture of ACN and aqueous formic acid solution (0.1%). Flow rates were set to 1 and 21 mL min^{-1}. All compounds tested displayed a purity of > 95% (254 nm).

Cell Cultures: HEK293 cells stably transfected with human *KCNT1* (herein referred to as HEK-Slack cells; SB-HEK-KCa4.1; SB Drug Discovery, Lanarkshire, UK) were maintained in Dulbecco's modified Eagle's medium-Glutamax with 10% fetal calf serum and 1% penicillin/streptomycin, supplemented with 0.6 mg mL^{-1} G-418 (all from Gibco/Thermo Fisher Scientific) in 5% CO_2 at 37 °C. Cells were passaged every 4–5 days from P11 to P35 depending on their confluence.

FluxOR Assay: To determine the Slack-activating efficacy and potency of the novel compounds, a commercial FluxOR potassium ion channel assay (#10 017; Invitrogen) was used. HEK-Slack cells were plated at a density of 50 000 cells per well on a poly-D-lysine coated (75 µg mL^{-1}, Sigma–Aldrich) 96-well, black-walled microplate with clear bottom (#655 090; Greiner Bio-One) in DMEM (100 µL per well) containing 10% FBS and 1% penicillin/streptomycin 24 h prior to assaying. In the initial experiments shown in Figure S3A–F (Supporting Information), HEK-Slack cells were plated at a density of 100 000 cells/well 48 h prior to the assay. On the day of the experiment, the cells were loaded with FluxOR dye according to the manufacturer's protocol. A Na^+-free assay buffer, adjusted to pH 7.4 with KOH, containing 140 mM choline chloride, 5 mM KCl, 2 mM $CaCl_2$, 2 mM $MgSO_4$, 10 mM HEPES, and 5.55 mM glucose was used. To reduce background fluorescence, all assay components were complemented with a 10% BackDrop Background Suppressor (#B10511; Invitrogen).

All compounds were prepared as a 333 mM stock in DMSO and diluted on the experimental day to a final concentration of 100, 50, 25, 12.5, 6.25, 3.125, or 1.5625 µM in an assay buffer with DMSO adjusted to 0.03%. Before treatment, the cells were washed, and the medium was exchanged for the assay buffer. In a total volume of 90 µL per well, the cells were then incubated for 30 min at 37 °C with compounds at the indicated concentrations, or 0.03% DMSO alone as the vehicle. A positive control with 50 µM loxapine was always conducted in parallel. Fluorescence was measured using an Infinite M200 microplate reader (Tecan) with excitation at 485 nm (9 nm bandwidth) and emission at 525 nm (20 nm bandwidth) in the bottom read mode. First, the baseline fluorescence of the individual wells was established. Thereafter cells were stimulated with 20 µL Tl_2SO_4 (5 mM) solution injected at 100 µL s^{-1}, and fluorescence was further recorded for 100 s. Assays were run in triplicate. For all time points, the ratio of fluorescence to baseline fluorescence was calculated first for individual wells, and the average was then used.

Dose-response curves comprising six concentrations were obtained in triplets using fluorescence/$\text{fluorescence}_{\text{Baseline}}$ ratios at the 100th s. Values were calculated relative to loxapine in each experiment as follows: $100 \times ([F/F_B(\text{Compound}) - F/F_B(\text{Vehicle}_{\text{mean}})]/[(F/F_B(\text{Loxapine}) - F/F_B(\text{Vehicle}_{\text{mean}})]$. To generate EC_{50} and E_{MAX} values, a standard, logistic, nonlinear regression analysis with GraphPad Prism 9.0 was used.

Patch-Clamp Recordings in HEK-Slack Cells: HEK-Slack cells were plated onto poly-D-lysine-coated (100 µg mL^{-1}, Sigma–Aldrich) coverslips 1 day before experiments and cultured in DMEM containing 10% FBS and 1% penicillin/streptomycin in 5% CO_2 at 37 °C. Whole-cell voltage-clamp recordings were acquired using an EPC 9 amplifier combined with Patchmaster software (HEKA Electronics, Lambrecht/Pfalz, Germany). Currents were sampled at 20 kHz and filtered at 5 kHz. Data analysis was performed using the Fitmaster software (HEKA Electronics). Membrane potential was held at −70 mV and outward K^+ current (I_K) was evoked by depolarizing steps (500 ms duration) ranging from −120 to +120 mV in increments of 20 mV. The pipette solution contained 140 mM KCl, 2 mM $MgCl_2$, 5 mM EGTA, and 10 mM HEPES and was adjusted to pH 7.4 with KOH. The extracellular solution contained 140 mM NaCl, 5 mM KCl, 2 mM $CaCl_2$, 2 mM $MgCl_2$, and 10 mM HEPES and was adjusted to pH 7.4 with NaOH. The osmolarity of all the solutions was adjusted to 290–300 mOsmol L^{-1} using glucose. Patch pipettes had a resistance of 6–8 MΩ and were obtained from borosilicate glass capillaries (Science Products) using a conventional puller (DMZ-Universal Puller, Zeitz Instruments). After baseline measurements, new compounds or loxapine solved in an external solution containing 0.03% DMSO (each with a final concentration of 50 µM)

were added to the bath without continuous perfusion, and K^+ currents were measured within 5 min. The fold-increase values in the patch-clamp experiments were determined by calculating the baseline current density relative to the current density after compound application.

In recordings with 10 mM pipette Na^+ (Figure S7, Supporting Information), the pipette solution contained 130 mM KCl, 10 mM NaCl, 2 mM $MgCl_2$, 5 mM EGTA, 10 mM HEPES and was adjusted to pH 7.4 with KOH. Compound 6 was solved in an external solution containing 0.03% DMSO with a final concentration of 25 µM in these experiments.

Patch-Clamp Recordings in DRG Neurons: To produce a primary cell culture of DRG neurons, naïve C57BL/6N mice (aged 4–8 weeks) were sacrificed by CO_2 inhalation, and lumbar (L1–L5) DRGs were transferred to a hanks' balanced salt solution (Gibco, Thermo Fisher Scientific). After incubation with 500 U mL^{-1} collagenase IV and 2.5 U mL^{-1} dispase II (both from Sigma Aldrich) for 60 min, including carefully shaking every 20 min, DRGs were washed and gently triturated twice with a fire-polished Pasteur pipette in neurobasal medium (Gibco, Thermo Fisher Scientific) including 10% FBS and 0.5 mM GlutMax (Gibco, Thermo Fisher Scientific). Dissociated DRGs were seeded onto poly-D-lysine-coated (100 µg mL^{-1}) coverslips and cultured in neurobasal medium supplemented with 2% B27 (Gibco, Thermo Fisher Scientific), 1% penicillin/streptomycin, and 0.5 mM GlutMax in 5% CO_2 at 37 °C.

For patch-clamp recordings shown in Figure 5, DRG cultures were incubated with an "inflammatory soup" (10 µM histamine, 10 µM PGE_2, 10 µM serotonin, and 10 µM bradykinin)[36] overnight in order to increase neuronal excitability. Before recording, DRG neurons were preincubated with 10 µg mL^{-1} Alexa Fluor 488-conjugated IB4 (Sigma–Aldrich) for 5–10 min to select Slack-expressing neurons. Whole-cell current-clamp recordings were obtained using an EPC 9 amplifier combined with Patchmaster software (HEKA Electronics, Lambrecht/Pfalz, Germany). General settings, pipettes, and extracellular solutions were used as described above. Evoked action potentials (APs) were elicited by 10 ms current injections starting at 0 pA in 20 pA increments to determine electrophysiological parameters. AP firing was induced by depolarizing current pulses (200–950 pA at 150 pA intervals, 1000 ms duration). Recordings were performed at baseline and following a 1 min incubation with 50 µM compound 6 or vehicle (external solution containing 0.03% DMSO). The number of APs before and after the compound application was counted at the same current-injection step.

For patch-clamp experiments presented in Figure S12 (Supporting Information), voltage-dependent Na^+ currents (I_{Na}) were recorded using a prepulse by −120 mV for 700 ms from a holding potential of −70 mV, followed by a 100 ms testpulse of −10 mV. Current-voltage (I-V) relations were recorded using a pulse protocol with 10 mV steps starting at −80 mV to +10 mV. The densities of the currents were determined by normalizing the peak current to cell capacitance. The pipette solution for I_{Na} measurement contained 110 mM CsF, 10 mM NaCl, 5 mM $MgCl_2$, 11 mM EGTA, 10 mM HEPES, and pH 7.2 adjusted with CsOH. The external solution contained 30 mM NaCl, 85 mM choline chloride, 5 mM KCl, 20 mM TEA-Cl, 0.1 mM $CaCl_2$, 5 mM $MgCl_2$, 10 mM HEPES, 5 mM glucose, pH 7.4 adjusted with NaOH. Tetrodotoxin-citrate (250 nM; Biotrend) solved in an external solution was added into the bath. DRG neurons were preincubated with 10 µg mL^{-1} Alexa Fluor 488-conjugated IB4 for 5–10 min to select Slack-expressing neurons. Recordings were performed at baseline and following either 50 µM compound 6, 50 µM lidocaine (Sigma–Aldrich), or vehicle (external solution containing 0.03% DMSO).

Cytotoxicity Multiplex Assay in HEK293T Cells: To assess cell viability, a live cell high-content screen was performed in HEK293T cells as described previously.[25] In brief, HEK293T cells (ATCC CRL-1573) were cultured in DMEM plus L-glutamine (high glucose) supplemented by 10% FBS (Gibco) and penicillin/streptomycin (Gibco). Cells were seeded at a density of 1500 cells/well in 384 well plates in culture medium (cell culture microplate, PS, f-bottom, µClear, 781 091; Greiner). Cells were stained simultaneously with 60 nM Hoechst33342 (Thermo Scientific), 75 nM Mitotracker red (Invitrogen), 0.3 µL per well annexin V Alexa Fluor 680 conjugate (Invitrogen), and 25 nL per well BioTracker 488 green microtubule cytoskeleton dye (EMD Millipore). The fluorescence and cellular shape were measured after 6 h of compound exposure using a CQ1 high-content confocal microscope (Yokogawa). The following setup parameters were used for image acquisition: Ex 405 nm/Em 447/60 nm, 500 ms, 50%; Ex 561 nm/Em 617/73 nm, 100 ms, 40%; Ex 488/Em 525/50 nm, 50 ms, 40%; bright field, 300 ms, 100% transmission, one centered field per well, 7 z stacks per well with 55 µm spacing. Images were analyzed using the CellPathfinder software (Yokogawa). Cells were detected and gated in different cell populations as described previously[47] using a machine learning-based algorithm. Briefly, compound precipitation was detected as Hoechst high-intensity objects. Cell viability was calculated based on the normal cell population (cells that did not show Hoechst high-intensity objects). Healthy cells were further gated into phenotypic subpopulations (membrane integrity and mitochondrial mass). The compounds were tested in duplicates. Cell counts of different populations were normalized against cells treated with 0.1% DMSO (100%).

Cytotoxicity Multiplex Assay in HEK-Slack Cells: The viability of HEK-Slack cells was assessed using bright-field microscopy. HEK-Slack cells were cultured in Dulbecco's modified Eagle's medium-GlutaMAX with 10% fetal calf serum and 1% penicillin/streptomycin, supplemented with 0.6 mg mL^{-1} G-418 (all from Gibco/Thermo Fisher Scientific). Cells were seeded at a density of 1200 cells/well in 384 well plates in culture medium (cell culture microplate, PS, f-bottom, µClear, 781 091; Greiner). Cell confluence was measured using the IncuCyte S3 (Satorius) over 24 h. Compounds were tested in biological duplicates. Cell confluence was normalized to cells treated with 0.1% DMSO (100%).

Metabolic Stability Assay: The solubilized test compound (5 µL, final concentration 10 µM) was preincubated at 37 °C in 432 µL phosphate buffer (0.1 M, pH 7.4) together with 50 µL NADPH regenerating system (30 mM glucose-6-phosphate, 4 U mL^{-1} glucose 6-phosphate dehydrogenase, 10 mM NADP, and 30 mM $MgCl_2$). After 5 min, the reaction started upon the addition of 13 µL of microsome mix from the liver of Sprague-Dawley rats (Invitrogen; 20 mg protein per mL in 0.1 M phosphate buffer) in a shaking water bath at 37 °C. The reaction was stopped by adding 500 µL ice-cold methanol at 0, 15, 30, and 60 min. The samples were centrifuged at 5000 × *g* for 5 min at 4 °C and the test compound was quantified from the supernatants by HPLC; the composition of the mobile phase was adapted to the test compound in a range of MeOH 40–90% and water (0.1% formic acid) 10–60%. Flow rate: 1 mL min^{-1}; stationary phase: Purospher STAR, RP18, 5 µm, 125 × 4; precolumn: Purospher STAR, RP18, 5 µm, 4 × 4; detection wavelength: 254 and 280 nm; injection volume: 50 µL. Control samples were used to evaluate the stability of the test compounds in the reaction mixture. The first control was without NADPH, which is needed for the enzymatic activity of the microsomes, the second control was with inactivated microsomes (incubated for 20 min at 90 °C), and the third control was without the test compound (to determine the baseline). The amounts of test compounds were quantified using an external calibration curve.

Dopamine D_2/D_3 Receptor Affinity Assay: CHO cells stably expressing human dopamine D_{2short} (D_2R) and D_3 receptor (D_3R) were washed and harvested using PBS. Cells were centrifuged (3000 × *g*, 10 min, 4 °C) and homogenized with an Ultraturrax homogenizer in ice-cold D_2/D_3R binding buffer (10 mM $MgCl_2$, 10 mM $CaCl_2$, 5 mM KCl, 120 mM NaCl, and 50 mM Tris, pH 7.4). The cell membrane homogenate was centrifuged (20 000 × *g*, 20 min, 4 °C), and the resulting cell pellet was resuspended in the binding buffer. Crude membrane extracts were kept at −80 °C until use. Before starting the experiments, cell membranes were thawed, homogenized by sonication (3 × 10 s), and stored in an ice-cold binding buffer. For radioligand binding assays, membrane extracts (25 and 20 µg per well in a final volume of 0.2 mL binding buffer for D_2R and D_3R, respectively) were incubated with [^{3}H]-spiperone (0.2 nM final concentration) and various concentrations of the test ligand for 120 min at room temperature. Assays were performed at least in triplicate with appropriate concentrations ranging from 0.01 nM to 100 µM of the test compound. Non-specific binding was determined using 10 µM haloperidol. By filtering through GF/B filters pretreated with 0.3% (m/v) polyethyleneimine, the bound radioligand was separated from free radioligand using a cell harvester. Radioactivity was measured using liquid scintillation counting. Data were evaluated using the GraphPad Prism 9 software (San Diego, CA, USA) with a nonlinear regression fit.

Histamine H_1 Receptor Affinity Assay: For membrane preparations of CHO cells stably expressing the human histamine H_1 receptor (H_1R), cells were washed and harvested with PBS buffer, homogenized by sonication (3 × 15 s) in ice-cold HEPES-H_1R binding buffer (20 mM HEPES, 10 mM $MgCl_2$, and 100 mM NaCl), followed by a centrifugation step (20 000 × *g*, 30 min, 4 °C). The resulting cell pellet was resuspended in binding buffer and homogenized using a hand potter. Membrane extracts were stored at −80 °C. Prior to use, the membranes were handled as described for D_2R/D_3R. For radioligand binding assays, membranes (40 µg per well in a final volume of 0.2 mL binding buffer) were incubated with [^{3}H]-pyrilamine (1 nM final concentration) and different concentrations of test ligand for 120 min at room temperature. Assays were performed at least in duplicates with appropriate concentrations between 0.1 nM and 100 µM of the test compound. Nonspecific binding was determined using 10 µM chlorphenamine maleate. The subsequent procedure was performed as described for D_2R/D_3R.

Slack Expression and Purification: The gene encoding isoform 1 of human Slack (*KCNT1*; NCBI ref. seq. NM_02 0822.3, residues 1–1235) were cloned into the mammalian overexpression vector pcDNA3.1 (Clontech) together with a green fluorescent protein and a twin strep-II-tag sequence for affinity purification at the C-terminus. A TEV protease cleavage sequence was included between the Slack and the GFP sequences to remove the tags. For large-scale expression, HEK293F cells were transiently transfected with the Slack-encoding plasmid using polyethylenimine (PEI) (DNA to PEI ratio of 1:3) and grown in a Freestyle medium (Thermo Fischer). Seventy-two hours post-transfection, the cells were harvested by centrifugation at 1000 × *g* for 5 min. Subsequently, the cells were resuspended in ice-cold homogenization buffer (20 mM HEPES, pH 7.6, 350 mM KCl, 10 mM $CaCl_2$, 10 mM $MgCl_2$, and 5 mM DTT) supplemented with 1× complete protease inhibitor mix (Serva), 1% (w/v) DDM, 0.1% (w/v) CHS (Anatrace), and 100 mU benzonase. Solubilization was done for 120 min on an overhead rotator at 4 °C. The lysate was centrifuged at 100 000 × *g* for 1 h and 4 °C to remove the insolubilized membranes and cell debris. The supernatant was then batch-incubated with 250 µL bed volume per L cell culture of Strep-Tactin agarose (IBA Lifesciences) pre-equilibrated with wash buffer (20 mM HEPES, pH 7.6, 350 mM KCl, 10 mM $MgCl_2$, 1× complete protease inhibitor mix, 0.1% (w/v) DDM, 0.01% (w/v) CHS, and 100 µg mL^{-1} bovine brain lipids (BBL)) for 4 h at 4 °C. The beads were then collected on a gravity flow column and washed thrice with ten-column volumes of ice-cold wash buffer. The remaining protein was digested with TEV protease (20:1 w/w ratio) on the column overnight at 4 °C to remove the affinity tag and then eluted with two column volumes of wash buffer. The eluate was concentrated to 500 µL using an Amicon Ultra-15 (Merck Millipore) and further purified by size-exclusion chromatography on a Superdex 200 10/300 column (GE Life Sciences) in SEC buffer (20 mM HEPES pH 7.6, 350 mM KCl, 0.05% DDM, and 10 µg mL^{-1} BBL). Peak fractions were pooled and concentrated to 5 µM (0.7 mg mL^{-1}) final concentration using an Amicon Ultra-15 (Merck Millipore) for further analysis.

Differential Scanning Fluorometry (DSF): The melting temperature was determined from the fluorescence of 7-diethylamino-3-(4-maleimidophenyl)−4-methylcoumarin (CPM) dye. A total of 22.5 µL of 5 µM Slack in SEC buffer was mixed with 22.5 µL of the compounds (compound 6, loxapine, or Slack-inhibiting compound 31 from ref. [27]) diluted in SEC buffer in the range of 0–200 µM and incubated at 4 °C for 4 h. Five microliters of the CPM dye (15 µg mL^{-1} CPM final concentration) in the SEC buffer was added to the protein compound mixture and further incubated for 30 min on ice in the dark. The samples were centrifuged at 15 000 × *g* at 4 °C for 10 min to remove aggregates. Melting curves were recorded in an RT-PCR (Thermo Fischer) using a temperature range of 10–80 °C in 1 °C-increments, increasing every 75 s. The CPM dye was excited at a wavelength of 365 nm and the emission was measured at 470 nm.

In Vitro Safety Panel: A SafetyScreen44 panel was conducted by Eurofins Cerep (Celle l' Evescault, France; item P270) to identify interactions with 44 preselected pharmacological targets. Loxapine and compound 6 were tested at 10 µM. Measurements were performed in duplicate. The results are expressed as the percent inhibition of control-specific binding obtained in the presence of the test compounds.

Pharmacokinetics: Pharmacokinetic experiments were performed by Bienta (Enamine Biology Services, Kiev, Ukraine). Study design, animal selection, handling, and treatment were performed in accordance with the Enamine PK study protocols and the Institutional Animal Care and Use Guidelines. Male C57BL/6J mice (11–16 weeks old) were used in this study. The animals were fasted for 4 h before dosing. Compounds (loxapine succinate or compound 6 hydrochloride; dissolved in a solution of 25% 2-hydroxypropyl-β-cyclodextrin in saline) were administered via the i.p., p.o., or i.v. route, and blood and brain tissue were taken at different time points thereafter (0.25, 0.5, 1, 2, and 4 h after i.p. administration; 0.25, 0.5, 1, 2, 4, and 8 h after p.o. administration; 0.083, 0.25, 0.5, 1, 2, and 4 h after i.v. administration). Each timepoint treatment group included three animals, and a control group was employed, including one animal.

Before collecting blood and brain tissue, the mice were anesthetized with 2,2,2-tribromoethanol (150 mg kg^{-1} i.p.). In studies with i.p. compound administration, the chest was opened, an incision was made in the right atrium, whole blood was collected into tubes containing K2EDTA, and the animals were perfused with saline (10 mL) prior to the excision of the brain tissue (left lobe). In studies with p.o. or i.v. delivery of compounds, blood was collected from the orbital sinus in microtainers containing K3EDTA, the animals were sacrificed by cervical dislocation, and the brain tissue (left lobe) was excised. After collection, the blood samples were centrifuged for 10 min at 3000 rpm, and the brain samples were weighed. All samples were immediately processed, flash-frozen, and stored at −70 °C until subsequent analysis.

The compound levels in the plasma and brain samples were determined using liquid chromatography–tandem mass spectrometry (LC-MS/MS) by a staff member from Bienta. Pharmacokinetic data analysis was performed using non-compartmental, bolus injection, or extravascular input analysis models with WinNonlin 5.2 (PharSight). Data below the lower limit of quantitation were presented as missing data to improve the validity of the half-life calculations. For each treatment condition, the final concentration values obtained at each time point were analyzed for outliers using Grubbs' test, with the level of significance set at $p < 0.05$. The sum of the $AUC_{0\text{-inf}}$ (area under the concentration-time curve from zero to time infinity) was used to estimate the $ratio_{brain/plasma}$ (concentration ratio of the compound in the brain and plasma).

Animals for Behavioral Tests: Experiments were performed in 8–16 week-old C57BL/6N mice (Charles River, Sulzfeld, Germany) and Slack$^{-/-}$ mice[24] of either sex. The animals were housed under a 12 h light/dark cycle with access to food and water ad libitum. All experiments adhered to the Animal Research: Reporting on In Vivo Experiments (ARRIVE) guidelines and were approved by and conducted in accordance with the regulations of the local Animal Welfare authorities (Regierungspräsidium Darmstadt, Germany; approval number V54-19c20/15-FR/1013 and FR/2011). All behavioral studies were conducted during the light cycle of the day at room temperature (20–24 °C) by an observer blinded for the treatment of the animals and/or their genotype.

Accelerating Rotarod and Vertical Pole Test: Mice were placed on a rotarod treadmill (Ugo Basile, Italy) at increasing speed (4–40 rpm over 300 s) and trained for 4–5 consecutive days. Only mice that reached 300 s without falling off during the training sessions were included in the experiment. In the vertical pole test, the mice were placed head-upward on top of a vertical pole with a rough surface (diameter, 1 cm; height, 40 cm), and the time until the animals reached the ground was recorded (cut-off time 20 s). Only mice that reached the ground within 10 s in the baseline measurements were included in the experiment. After baseline measurements without compound administration, compound 6 hydrochloride, loxapine succinate or vehicle (10% 2-hydroxypropyl-β-cyclodextrin (ITW Reagents) in 0.9% saline; used for compound 6, loxapine, and morphine in all behavioral tests in this study) were i.p. administered, and 15 min later, the accelerating rotarod followed by the vertical pole test were performed. The means of three trials at each time point were calculated for further analyses.

Acute Itch Behavior: Three to four days before the day of the experiment, the fur on the dorsolateral aspect of the neck was shaved under brief isoflurane anesthesia. On the testing day, the mice were habituated to a Plexiglas cylinder (30 cm in diameter) for 30 min. Compound 6

hydrochloride or vehicle were i.p. or p.o. administered, and 15 min later, the pruritogens chloroquine (200 µg), SLIGRL (100 µg), β-alanine (100 µg), or histamine (800 µg), all dissolved in 0.9% saline (20 µL), were injected subcutaneously into the nape of the neck.[29] Number of scratching bouts directed toward the nape of the neck was assessed over 30 min by videotaping. In experiments with the Slack inhibitor, compound 31 (ref. [27]; 30 mg kg^{-1} in 0.9% NaCl with 2% DMSO and 10% Kolliphor) was i.p. administered 5 min prior to compound 6.

Allergic Contact Dermatitis Model: To induce persistent itch, a model of allergic contact dermatitis[32] was used. The fur on the dorsolateral aspect of the neck was shaved under brief isoflurane anesthesia. Three to four days later, the shaved skin area was exposed to 100 µL of 0.15% 2,4-dinitrofluorobenzene (DNFB) in acetone/olive oil (3:1). After 10–11 days, the skin was shaved again, and the DNFB solution was applied 3–4 days later (i.e., two painting sessions 14 days apart). Ninety minutes after the second DNFB application, the mice were habituated to a plexiglass cylinder (30 cm diameter) for 15 min. Compound 6 hydrochloride or vehicle was administered i.p., and 15 min later, spontaneous scratching was recorded over 30 min by videotaping.

Atopic Dermatitis Model: Chronic itching was induced using the MC903 model.[48] The fur on the dorsolateral aspect of the neck was shaved under brief isoflurane anesthesia. Five days later, 20 µL MC903 (0.2 mM; Calcipotriol, Tocris) solved in absolute ethanol was applied to the skin at the back of the neck under brief anesthesia for 7 consecutive days. On day 8, the mice were habituated for 30 min in a plexiglass cylinder (30 cm in diameter). Compound 6 hydrochloride or vehicle was administered i.p., and 15 min later, spontaneous scratching was recorded over 30 min by videotaping.

Pulse Oximetry: To measure cardiovascular function, a pulse oximeter (MouseOX Plus, Starr Life Sciences Corp.) was used in conscious, freely moving mice. After three consecutive days of habituating the mice to the collar clip for at least 30 min, baseline measurements were performed. Compounds (compound 6 hydrochloride, loxapine succinate, or morphine sulfate pentahydrate) or vehicle were i.p. administered, and after a resting time of 5 min, the heart rate, respiratory rate, and arterial O_2 saturation were recorded over 30 min. All the datasets were sampled at 1 Hz, error-corrected according to the manufacturer's instructions, and averaged over 300 s for each time point.

Hargreaves Test: Mice were placed in plastic chambers on a heated glass panel (32 °C) of a Plantar Test device (Hargreaves method; IITC Life Science, CA) and acclimated for 1 h. An infrared heat source (intensity set to 25) was applied to the plantar surface of the hind paw, and the time until the animal elicited a withdrawal response was determined. Each hind paw was measured 4–5 times with a minimum interval of 20 s between measurements, and the mean value was calculated. Measurements that reached the cutoff time (20 s) were excluded. Thermal sensitivity was assessed at baseline and 15 min after i.p. administration of compound 6 hydrochloride or vehicle.

Von Frey Filament Test: The mice were placed in plastic chambers on a wire mesh grid and acclimated for 1 h. Mechanical sensitivity was assessed using von Frey filaments (Ugo Basile) with increasing forces (0.04, 0.07, 0.16, 0.4, 0.6, 1, 1.4, 2, and 4 g) applied to the plantar surface of the hind paw. A withdrawal response within 1 s of a slight hair bending was recorded as a positive reaction. Each filament was applied 10 times within 10 min and both hind paws were measured equally. The total number of responses per force was recorded as the percentage of withdrawals per mouse. After baseline measurement, compound 6 hydrochloride or vehicle was administered intraperitoneally, and 15 min later, a second measurement was performed.

Statistical Analysis: Statistical analysis was performed using Prism 9 (GraphPad). No statistical methods were used to pre-determine the sample sizes; however, the sample sizes were similar to those reported in previous publications[29,31,32,34] and standard practices in the field. Kolmogorov–Smirnov or Shapiro–Wilk tests were used to assess the normal distribution of data within groups. Normally distributed data were analyzed using two-tailed unpaired or paired t-test, one-way-ANOVA, or two-way MC ANOVA and are expressed as the mean ± standard error of the mean (SEM) or single data points with the mean ± SEM. Non-parametric data were analyzed using a two-tailed Mann–Whitney test or Kruskal–Wallis test and presented as single data points with medians and interquartile ranges. Outliers were identified using the ROUT method (Q = 1%), and one outlier was excluded from the analysis (patch-clamp recording with 0 mM Na^+ in Figure S7, Supporting Information) in the entire study. For all statistical tests, a probability value of $p < 0.05$ was considered statistically significant. Asterisks in the figures indicate: $^{*}p < 0.05$, $^{**}p < 0.01$, and $^{***}p < 0.001$. Data from FluxOR experiments shown in Figure 1A were analyzed by applying a standard, logistic, nonlinear regression implemented in Prism 9 to get dose-response curves representing EC_{50} and E_{MAX} values ± 95% CI. Data from FluxOR experiments shown in Figure 1A and Figure S3A–G (Supporting Information) and from DSF experiments shown in Figure S6B (Supporting Information) are presented as mean ± SD. In the in vivo experiments, behavioral tests were performed by observers blinded to the treatment groups or genotypes. The treatment groups were randomized and evenly distributed across cages and sexes. Details of the analyses, including the statistical test, post-hoc test, number of replicates for each analysis, and number of animals per group, are indicated in the figure legends.

Supporting Information

Supporting Information is available from the Wiley Online Library or from the author.

Acknowledgements

The authors thank Astrid Kaiser, Sylvia Oßwald, and Cyntia Schäfer for excellent technical assistance. This work was supported by a grant from the Else Kröner-Fresenius-Stiftung (project 2018_A95; to A.S. and E.P.). R.Lu received funding from the Deutsche Forschungsgemeinschaft (LU 2514/1-1) for related work on Slack potassium channels. A.M., S.K., and S.M. are grateful for support from the Structural Genomics Consortium (SGC), a registered charity (No: 1097737) that received funds from Bayer AG, Boehringer Ingelheim, Bristol Myers Squibb, Genentech, Genome Canada through Ontario Genomics Institute, Janssen, Merck KGaA, Pfizer, and Takeda, and by the German Cancer Research Center (DKTK) and the Frankfurt Cancer Institute (FCI). A.M. is supported by the SFB 1177 "Molecular and Functional Characterization of Selective Autophagy". S.M. receives funding from the ICR. The CQ1 microscope was funded by FUGG (INST 161/920-1 FUGG). H.S., A.F., and M.D. are grateful for support by DFG GRK 2158.

Open access funding enabled and organized by Projekt DEAL.

Conflict of Interest

This work is related to patent application #EP23160797.9 'Slack-activating compounds and their medical use', of which A.B., W.F.Z, C.F., V.H.-O., J.H., R. Lu, D.S., E.P., and A.S. are co-inventors. All other authors declare no conflict of interest.

Author Contributions

A.B. and W.F.Z. are first authors which contributed equally to this work, and that E.P. and A.S. are last authors which contributed equally to this work. A.B. performed FluxOR assays, electrophysiological recordings, and in vivo experiments, analyzed data, prepared the figures, and assisted with preparing the manuscript. W.F.Z. designed and synthesized compounds and assisted with preparing the manuscript. C.F. established the FluxOR assay, performed initial FluxOR and in vivo experiments, and analyzed these data. V.H.-O. designed and synthesized compounds. J.H. established and supervised the FluxOR assay. S.S. and I.H. performed and/or evaluated DSF analyses. M.D., A.F., and H.S. performed dopamine and histamine binding assays. A.M., S.K., and S.M. conducted and/or evaluated cytotoxicity measurements. M.H. assisted in electrophysiological

recordings. K.M. supervised the electrophysiological recordings. R.Lu performed in vivo experiments. R.Lukowski and P.R. provided Slack knockout mice and analytical tools. D.S. contributed to the conceptualization of the project and edited the manuscript. H.S. conceived the project. E.P. conceived the project, supervised compound design and synthesis, analyzed data, and wrote the manuscript. A.S. conceived the project, designed and supervised the in vivo experiments, analyzed data, and wrote the manuscript. All authors revised and approved the manuscript.

Data Availability Statement

The data that support the findings of this study are available in the supplementary material of this article.

Keywords

drug development, itch, kcnt1, slack, target validation

Received: September 29, 2023
Revised: January 15, 2024
Published online:

[1] E. Carstens, T. Follansbee, M. I. Carstens, *Acta Derm. Venereol.* **2020**, *100*, 2.
[2] F. Wang, B. S. Kim, *Immunity* **2020**, *52*, 753.
[3] K. Rossbach, C. Nassenstein, M. Gschwandtner, D. Schnell, K. Sander, R. Seifert, H. Stark, M. Kietzmann, W. Baumer, *Neuroscience* **2011**, *190*, 89.
[4] B. S. Kim, *Neuron* **2022**, *110*, 2209.
[5] M. E. Kopyciok, H. F. Stander, N. Osada, S. Steinke, S. Stander, *Acta Derm. Venereol.* **2016**, *96*, 50.
[6] U. Matterne, C. J. Apfelbacher, A. Loerbroks, T. Schwarzer, M. Buttner, R. Ofenloch, T. L. Diepgen, E. Weisshaar, *Acta Derm. Venereol.* **2011**, *91*, 674.
[7] S. Inan, N. J. Dun, A. Cowan, *Molecules* **2021**, *26*, 5517.
[8] A. Vander Does, T. Ju, N. Mohsin, D. Chopra, G. Yosipovitch, *Pharmacol. Ther.* **2023**, *243*, 108355.
[9] X. J. Chen, Y. G. Sun, *Nat. Commun.* **2020**, *11*, 3052.
[10] D. Usoskin, A. Furlan, S. Islam, H. Abdo, P. Lonnerberg, D. Lou, J. Hjerling-Leffler, J. Haeggstrom, O. Kharchenko, P. V. Kharchenko, S. Linnarsson, P. Ernfors, *Nat. Neurosci.* **2015**, *18*, 145.
[11] J. Meixiong, X. Dong, *Annu. Rev. Genet.* **2017**, *51*, 103.
[12] C. Tsantoulas, S. B. McMahon, *Trends Neurosci.* **2014**, *37*, 146.
[13] N. N. Knezevic, A. Yekkirala, T. L. Yaksh, *Anesth. Analg.* **2017**, *125*, 1714.
[14] A. Yuan, C. M. Santi, A. Wei, Z. W. Wang, K. Pollak, M. Nonet, L. Kaczmarek, C. M. Crowder, L. Salkoff, *Neuron* **2003**, *37*, 765.
[15] G. Budelli, Q. Sun, J. Ferreira, A. Butler, C. M. Santi, L. Salkoff, *J. Biol. Chem.* **2016**, *291*, 7347.
[16] R. Lu, K. Metzner, F. Zhou, C. Flauaus, A. Balzulat, P. Engel, J. Petersen, R. Ehinger, A. Bausch, P. Ruth, R. Lukowski, A. Schmidtko, *Int. J. Mol. Sci.* **2021**, *22*, 405.
[17] N. Sharma, K. Flaherty, K. Lezgiyeva, D. E. Wagner, A. M. Klein, D. D. Ginty, *Nature* **2020**, *577*, 392.
[18] P. L. Martinez-Espinosa, J. Wu, C. Yang, V. Gonzalez-Perez, H. Zhou, H. Liang, X. M. Xia, C. J. Lingle, *Elife* **2015**, *4*, 10013.
[19] J. Kupari, D. Usoskin, M. Parisien, D. Lou, Y. Hu, M. Fatt, P. Lonnerberg, M. Spangberg, B. Eriksson, N. Barkas, P. V. Kharchenko, K. Lore, S. Khoury, L. Diatchenko, P. Ernfors, *Nat. Commun.* **2021**, *12*, 1510.
[20] D. Tavares-Ferreira, S. Shiers, P. R. Ray, A. Wangzhou, V. Jeevakumar, I. Sankaranarayanan, A. M. Cervantes, J. C. Reese, A. Chamessian, B. A. Copits, P. M. Dougherty, R. W. t. Gereau, M. D. Burton, G. Dussor, T. J. Price, *Sci. Transl. Med.* **2022**, *14*, eabj8186.
[21] B. Biton, S. Sethuramanujam, K. Picchione, A. Bhattacharjee, N. Khessibi, F. Chesney, C. Lanneau, O. Curet, P. Avenet, *J. Pharmacol. Exp. Ther.* **2011**, *340*, 706.
[22] A. Chakrabarti, A. Bagnall, P. Chue, M. Fenton, V. Palaniswamy, W. Wong, J. Xia, *Cochrane Database Syst. Rev.* **2007**, CD001943, https://doi.org/10.1002/14651858.CD001943.pub2.
[23] S. Schmiedl, D. Peters, O. Schmalz, A. Mielke, T. Rossmanith, S. Diop, M. Piefke, P. Thurmann, A. Schmidtko, *Front. Pharmacol.* **2019**, *10*, 838.
[24] R. Lu, A. E. Bausch, W. Kallenborn-Gerhardt, C. Stoetzer, N. Debruin, P. Ruth, G. Geisslinger, A. Leffler, R. Lukowski, A. Schmidtko, *J. Neurosci.* **2015**, *35*, 1125.
[25] A. Tjaden, A. Chaikuad, E. Kowarz, R. Marschalek, S. Knapp, M. Schroder, S. Muller, *Molecules* **2022**, *27*, 1439.
[26] D. Popovic, P. Nuss, E. Vieta, *Ann. Gen. Psychiatry* **2015**, *14*, 15.
[27] A. M. Griffin, K. M. Kahlig, R. J. Hatch, Z. A. Hughes, M. L. Chapman, B. Antonio, B. E. Marron, M. Wittmann, G. Martinez-Botella, *ACS Med. Chem. Lett.* **2021**, *12*, 593.
[28] Y. C. Wong, S. K. Wo, Z. Zuo, *J. Pharm. Biomed. Anal.* **2012**, *58*, 83.
[29] Q. Liu, Z. Tang, L. Surdenikova, S. Kim, K. N. Patel, A. Kim, F. Ru, Y. Guan, H. J. Weng, Y. Geng, B. J. Undem, M. Kollarik, Z. F. Chen, D. J. Anderson, X. Dong, *Cell* **2009**, *139*, 1353.
[30] Q. Liu, H. J. Weng, K. N. Patel, Z. Tang, H. Bai, M. Steinhoff, X. Dong, *Sci. Signal.* **2011**, *4*, ra45.
[31] Q. Liu, P. Sikand, C. Ma, Z. Tang, L. Han, Z. Li, S. Sun, R. H. LaMotte, X. Dong, *J. Neurosci.* **2012**, *32*, 14532.
[32] A. Kitamura, R. Takata, S. Aizawa, H. Watanabe, T. Wada, *Sci. Rep.* **2018**, *8*, 5988.
[33] M. Li, P. Hener, Z. Zhang, S. Kato, D. Metzger, P. Chambon, *Proc. Natl. Acad. Sci. USA* **2006**, *103*, 11736.
[34] T. Voisin, C. Perner, M. A. Messou, S. Shiers, S. Ualiyeva, Y. Kanaoka, T. J. Price, C. L. Sokol, L. G. Bankova, K. F. Austen, I. M. Chiu, *Proc. Natl. Acad. Sci. USA* **2021**, *118*, e2022087118.
[35] E. C. Emery, P. Ernfors, (Ed.: J. N. W), Oxford University Press **2018**.
[36] L. Grundy, A. M. Harrington, J. Castro, S. Garcia-Caraballo, A. Deiteren, J. Maddern, G. Y. Rychkov, P. Ge, S. Peters, R. Feil, P. Miller, A. Ghetti, G. Hannig, C. B. Kurtz, I. Silos-Santiago, S. M. Brierley, *JCI Insight* **2018**, *3*, e121841.
[37] T. J. Tamsett, K. E. Picchione, A. Bhattacharjee, *J. Neurosci.* **2009**, *29*, 5127.
[38] M. O. Nuwer, K. E. Picchione, A. Bhattacharjee, *J. Neurosci.* **2010**, *30*, 14165.
[39] F. Huang, X. Wang, E. M. Ostertag, T. Nuwal, B. Huang, Y. N. Jan, A. I. Basbaum, L. Y. Jan, *Nat. Neurosci.* **2013**, *16*, 1284.
[40] C. G. Wermuth, *J. Med. Chem.* **2004**, *47*, 1303.
[41] C. G. Wermuth, *Drug Discov. Today* **2006**, *11*, 160.
[42] B. Zou, H. Yu, J. J. Babcock, P. Chanda, J. S. Bader, O. B. McManus, M. Li, *Assay Drug Dev. Technol.* **2010**, *8*, 743.
[43] T. Yamaguchi, T. Nagasawa, M. Satoh, Y. Kuraishi, *Neurosci. Res.* **1999**, *35*, 77.
[44] A. Zeisel, H. Hochgerner, P. Lonnerberg, A. Johnsson, F. Memic, J. van der Zwan, M. Haring, E. Braun, L. E. Borm, G. L. Manno, S. Codeluppi, A. Furlan, K. Lee, N. Skene, K. D. Harris, J. Hjerling-Leffler, E. Arenas, P. Ernfors, U. Marklund, S. Linnarsson, *Cell* **2018**, *174*, 999.
[45] J. Meixiong, C. Vasavda, S. H. Snyder, X. Dong, *Proc. Natl. Acad. Sci. USA* **2019**, *116*, 10525.
[46] B. A. Cole, S. J. Clapcote, S. P. Muench, J. D. Lippiat, *Trends Pharmacol. Sci.* **2021**, *42*, 700.
[47] A. Tjaden, R. T. Giessmann, S. Knapp, M. Schroder, S. Muller, *STAR Protoc.* **2022**, *3*, 101791.
[48] R. Z. Hill, M. C. Loud, A. E. Dubin, B. Peet, A. Patapoutian, *Nature* **2022**, *607*, 104.

